A Land-Plant-Specific Glycerol-3-Phosphate Acyltransferase Family in Arabidopsis: Substrate Specificity, sn -2 Preference, and Evolution

Weili Yang, Jeffrey P Simpson, Yonghua Li-Beisson, Fred Beisson, Mike Pollard, John B Ohlrogge

A Land-Plant-Specific Glycerol-3-Phosphate Acyltransferase Family in Arabidopsis: Substrate Specificity, *sn*-2 Preference, and Evolution[1][W][OA]

Weili Yang, Jeffrey P. Simpson, Yonghua Li-Beisson[2], Fred Beisson[2], Mike Pollard, and John B. Ohlrogge*

Department of Plant Biology, Michigan State University, East Lansing, Michigan 48824

Arabidopsis (*Arabidopsis thaliana*) has eight glycerol-3-phosphate acyltransferase (GPAT) genes that are members of a plant-specific family with three distinct clades. Several of these GPATs are required for the synthesis of cutin or suberin. Unlike GPATs with *sn*-1 regiospecificity involved in membrane or storage lipid synthesis, GPAT4 and -6 are unique bifunctional enzymes with both *sn*-2 acyltransferase and phosphatase activity resulting in 2-monoacylglycerol products. We present enzymology, pathway organization, and evolutionary analysis of this GPAT family. Within the cutin-associated clade, GPAT8 is demonstrated as a bifunctional *sn*-2 acyltransferase/phosphatase. GPAT4, -6, and -8 strongly prefer C16:0 and C18:1 ω-oxidized acyl-coenzyme As (CoAs) over unmodified or longer acyl chain substrates. In contrast, suberin-associated GPAT5 can accommodate a broad chain length range of ω-oxidized and unsubstituted acyl-CoAs. These substrate specificities (1) strongly support polyester biosynthetic pathways in which acyl transfer to glycerol occurs after oxidation of the acyl group, (2) implicate GPAT specificities as one major determinant of cutin and suberin composition, and (3) argue against a role of *sn*-2-GPATs (Enzyme Commission 2.3.1.198) in membrane/storage lipid synthesis. Evidence is presented that GPAT7 is induced by wounding, produces suberin-like monomers when overexpressed, and likely functions in suberin biosynthesis. Within the third clade, we demonstrate that GPAT1 possesses *sn*-2 acyltransferase but not phosphatase activity and can utilize dicarboxylic acyl-CoA substrates. Thus, *sn*-2 acyltransferase activity extends to all subbranches of the Arabidopsis GPAT family. Phylogenetic analyses of this family indicate that GPAT4/6/8 arose early in land-plant evolution (bryophytes), whereas the phosphatase-minus GPAT1 to -3 and GPAT5/7 clades diverged later with the appearance of tracheophytes.

sn-Glycerol-3-phosphate 1-*O*-acyltransferase (GPAT; Enzyme Commission [EC] 2.3.1.15) is the first enzyme in the pathway for the de novo synthesis of membrane and storage lipids. It catalyzes the transfer of an acyl group from acyl-CoA or acyl-ACP to the *sn*-1 position of *sn*-glycerol-3-phosphate (G3P). This reaction has been extensively characterized in bacteria, fungi, animals, and plants (Murata and Tasaka, 1997; Zheng and Zou, 2001; Gimeno and Cao, 2008; Zhang and Rock, 2008; Wendel et al., 2009; Chen et al., 2011a). In the Arabidopsis (*Arabidopsis thaliana*) genome, there are 10 genes annotated as GPATs. One of these is the soluble, plastid-localized GPAT (At1g32200) that utilizes acyl-ACP substrates and exhibits *sn*-1 acyl transfer regiospecificity (Nishida et al., 1993). A second enzyme is GPAT9 (At5g60620), which is localized to the endoplasmic reticulum (Gidda et al., 2009) and may be an acyl-CoA-dependent *sn*-1 GPAT that enables nonplastid glycerolipid synthesis. The remaining eight GPATs cluster together in a family (Zheng et al., 2003; Beisson et al., 2007; Gidda et al., 2009) that is not required for membrane or storage lipid biosynthesis; instead, several members of the family clearly affect the composition and quantity of cutin or suberin (Beisson et al., 2012).

Cutin and suberin are extracellular lipid barriers deposited by certain types of plant cells. These insoluble polymers, and associated waxes, function to control water, gas, and ion fluxes and serve as physical barriers to protect plants from pathogen invasion (Kolattukudy, 2001; Schreiber, 2010; Ranathunge et al., 2011). From an evolutionary perspective, the appearance of these lipid barriers was likely a requirement for the adaptation of plants to a terrestrial environment (Rensing et al., 2008). ω-oxidized fatty acids and glycerol are usually major constituents of both polymers (Bernards, 2002; Graça and Santos, 2007; Pollard et al., 2008). The detailed structures of cutin and suberin polymers are still largely unknown (Pollard et al., 2008), but direct esterification of fatty acids to glycerol and to each other has been demonstrated in a

[1] This work was supported by the U.S. Department of Agriculture (grant no. 2005–35318–15419), the National Science Foundation (grant no. MCB–0615563), and Bayer CropScience. J.P.S. was the recipient of a Natural Sciences and Engineering Research Council of Canada postgraduate scholarship.

[2] Present address: Department of Plant Biology and Environmental Microbiology, Commissariat à l'Energie Atomique/Centre National de la Recherche Scientifique/Aix Marseille Université, 13108 Saint-Paul-lez-Durance, France.

* Corresponding author; e-mail ohlrogge@msu.edu.

The author responsible for distribution of materials integral to the findings presented in this article in accordance with the policy described in the Instructions for Authors (www.plantphysiol.org) is: John B. Ohlrogge (ohlrogge@msu.edu).

[W] The online version of this article contains Web-only data.

[OA] Open Access articles can be viewed online without a subscription.

www.plantphysiol.org/cgi/doi/10.1104/pp.112.201996

large number of partial depolymerization studies of cutin and suberin (Graça and Santos, 2007; Graça and Lamosa, 2010). In Arabidopsis, GPAT4 and GPAT8 are required for the accumulation of C16 and C18 ω-hydroxy fatty acid (ω-OHFA) and α,ω-dicarboxylic acid (DCA) cutin monomers in stems and leaves (Li et al., 2007a). GPAT6 is required for the incorporation of the following C16 monomers: 10,16-dihydroxypalmitate (10,16-diOH C16:0-FA), hexadecane-1,16-dioic acid (C16:0-DCA), and 16-hydroxypalmitate (16-OH C16:0-FA), into flower cutin (Li-Beisson et al., 2009). (For a fatty acid, the abbreviation used is Cm:n-FA, where m is the number of carbon atoms and n is the number of double bonds. The position and number of hydroxyl groups precedes this notation. The same nomenclature is used for DCAs.) GPAT5 controls the accumulation of C22:0- and C24:0-FA, ω-OHFA, and DCA monomers in the suberin of roots and seed coats (Beisson et al., 2007). Recently, we demonstrated that GPAT4 and -6 are bifunctional enzymes that possess *sn*-2 acyltransferase and phosphatase activities (Yang et al., 2010) and that therefore produce *sn*-2 monoacylglycerols (MAGs) as the major product. GPAT5 also exhibits strong preference for *sn*-2 acylation but lacks phosphatase activity; thus, *sn*-2 lysophosphatidic acids (LPAs) are its major product (Yang et al., 2010).

These observations all attest to the fact that several members of the GPAT1 to -8 family are enzymatically very distinct from the GPATs required for membrane and storage lipid biosynthesis. Indeed, they represent a new acylglycerol biosynthesis pathway that provides precursors for cutin and suberin biosynthesis. To better understand the early steps in polyester synthesis and the roles contributed by GPAT4 to -8, and to determine whether the clade of GPAT1 to -3 has distinct or similar activity, we have characterized the regiochemistry and acyl substrate specificity of GPATs representing all three clades. We show that the cutin-associated GPAT8 is a bifunctional *sn*-2 acyltransferase/phosphatase, while GPAT1, an isozyme with uncertain function but important for tapetum and anther development (Zheng et al., 2003; Li et al., 2012), possesses *sn*-2 acyltransferase activity but not phosphatase activity. An important issue in defining the pathway of cutin/suberin biosynthesis is whether to place the P450 oxidation reactions before or after the G3P acylation reactions. As discussed (Pollard et al., 2008), previous evidence has not allowed definitive determination of the alternative pathways. However, conducting a GPAT substrate specificity study, particularly with a range of ω-oxidized and unmodified acyl-CoAs can help clarify the situation. Here, we show the acyl-CoA specificities of GPAT4, -5, -6, and -8 are concordant with the compositions of their respective cutins and suberins and the resulting changes in corresponding *gpat* mutants and overexpression lines. Furthermore, the results provide strong evidence that acyl transfer to glycerol by GPAT occurs after ω-oxidation of acyl chains, thus increasing our limited understanding of the biochemical pathway for cutin and suberin polymer assembly.

A phylogenetic analysis of Arabidopsis GPATs with vascular and nonvascular land-plant homologs provides an evolutionary view of the expansion and divergence of the gene family into three distinct clades that are associated with morphological and functional evolution and with the loss of phosphatase activity.

RESULTS

Synthesis of Substrates and Systems to Study GPAT Enzymology

Knowledge of the substrate specificity of the GPAT1 to -8 enzymes can contribute to understanding the role of these enzymes in determining cutin and suberin composition and the placement of their reaction in the biosynthetic pathway for polyester assembly. Determination of the acyl specificity of individual GPAT isoforms requires novel substrates and recombinant enzymes. Most of the ω-OHFAs and DCAs required for this study are not commercially available. Likewise, their acyl-CoA derivatives are unavailable and therefore were synthesized for this study. To obtain substrates representative of major cutin and suberin monomers, 10,16-diOH C16:0-FA, 18-hydroxyoleate (18-OH C18:1-FA), and 22-hydroxydocosanoate (22-OH C22:0-FA) were isolated from tomato (*Solanum lycopersicum*) peel powders, tobacco (*Nicotiana tabacum*) stigma lipids, and extractive-free cork (*Quercus suber*) powders, respectively. Greater than 95% purity for each was achieved by preparative thin-layer chromatography (TLC) and C18 reverse-phase HPLC. The above purified fatty acids along with commercially available 16-OH C16:0-FA, C16:0-DCA, octadec-9-cis-ene-1,18-dioate (C18:1-DCA), docosane-1,22-dioate (C22:0-DCA), and ricinoleate (12-OH C18:1-FA) were esterified to CoA by a carbonyldiimidazole-based synthesis (Kawaguchi et al., 1981). The structures of all synthesized acyl-CoAs with ω-OH or ω-COOH groups (C16:0, C18:1, and C22:0) were confirmed by electrospray ionization-mass spectrometry (ESI-MS) and ESI-MS/MS (for tandem mass spectrometry; Supplemental Table S1). The acyl-CoA substrates we have synthesized together with unmodified commercial acyl-CoAs (C16:0, C18:0, C18:1, C20:0, C22:0, and C24:0) provided a broad range of saturated and unsaturated acyl-CoAs, with and without ω- or mid-chain oxidation. Assays were in the linear range of product versus time and enzyme added. The yields from the synthesis of ω-oxidized acyl-CoAs were low (less than 200 nmol), preventing the determination of acyl-CoA K_m values and other kinetic properties of these GPATs.

The recombinant acyltransferase enzymes were prepared from microsomes isolated from GPAT-transformed yeast or from wheat germ in vitro translation products (prepared in the presence of liposomes; Yang et al., 2010). For assays in which the GPAT enzyme contains an active phosphatase domain, the yeast expression system produced both MAG and LPA

products, whereas the wheat germ-derived enzyme produced almost only MAG product with very little detectable LPA. For this study, we report activities for GPAT6 and -8 using enzymes from wheat germ translation, as they produce a simpler and more uniform product profile. We were unable to obtain active GPAT4 by wheat germ expression. This enzyme, and GPAT1 and -5, which do not have functional phosphatase domains and produce a simpler product profile, were assayed from yeast-expressed preparations.

GPAT8 Is an *sn*-2 Acyltransferase/Phosphatase and Prefers C16 and C18 ω-Oxidized Acyl-CoA Substrates

Previously, Li et al. (2007a) demonstrated that GPAT4 and GPAT8 are functionally redundant and required for Arabidopsis leaf and stem cutin production. Double knockouts (*gpat4/gpat8*) show a 60% to 70% reduction in C16 and C18 cutin monomers. Subsequent biochemical characterization of GPAT4 revealed that it has both *sn*-2 acyltransferase and phosphatase activity (Yang et al., 2010). To test if GPAT8 is another member of this class of novel *sn*-2 acyltransferases with an active phosphatase activity, the enzyme was assayed with C16:0 and C18:1 ω-OHFA or DCA acyl-CoAs. The reaction products were directly analyzed by borate-TLC to resolve *sn*-1 and *sn*-2 MAG isomers. GPAT8 products comigrated with ω-OH or DCA *sn*-2 MAGs (Fig. 1A). Since GPAT8 produces *sn*-2 MAGs as the major products (more than 90%; Fig. 1B), the results demonstrate that, together with GPAT4, both GPAT enzymes required for leaf and stem cutin biosynthesis are bifunctional *sn*-2 acyltransferases/phosphatases. The observed phosphatase activity of GPAT8 is consistent with its conservation of five key amino acids seen in motifs I and III of GPAT4 and GPAT6 phosphatase domains (Yang et al., 2010).

To determine substrate specificity, GPAT8 was assayed with both unsubstituted and ω-oxidized acyl-CoA substrates ranging from C16 to C24 carbon chain length (Fig. 2). GPAT8 acyl transfer activity was up to 10-fold higher with C16:0 and C18:1 ω-oxidized acyl-CoAs when compared with the unmodified acyl-CoAs. An exception to this generalization was for C16:0 DCA-CoA, which had low activity similar to C16:0-CoA. In addition, much lower or no activity was observed with either unsubstituted or ω-oxidized acyl groups with chain lengths longer than C18. GPAT4 also preferred ω-oxidized substrates, particularly DCAs, while activity was low with longer chain substrates (Supplemental Fig. S1).

GPAT6, Required for Cutin Biosynthesis in Flowers, Prefers C16 and C18 ω-Oxidized Acyl-CoA Substrates

Arabidopsis GPAT6 is highly expressed in flowers (more than 2-fold in petals and sepals above other GPATs). Analysis of *gpat6* knockout lines demonstrated

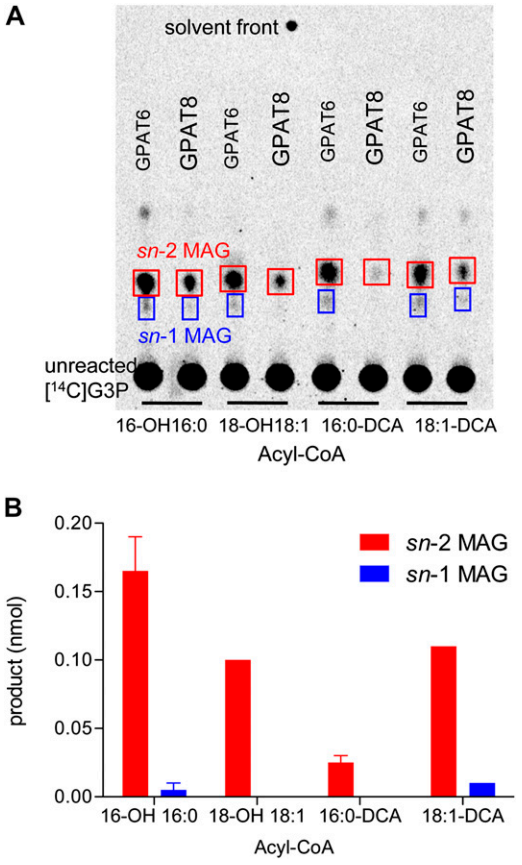

Figure 1. GPAT8 is a *sn*-2 acyltransferase. GPAT8 enzyme produced with the wheat germ cell-free translation system was assayed with 16-OH C16:0-CoA, 18-OH C18:1-CoA, C16:0-DCA-CoA, or C18:1-DCA-CoA as acyl donor and [^{14}C]G3P as acyl acceptor. A, Representative radio-TLC image of regiospecificity of ω-oxidized MAGs formed in GPAT8 assays. MAGs from GPAT8 assays were identified by comparison with R_f value of MAGs generated from parallel GPAT6 assays. The large spots at the origin are unreacted [^{14}C]G3P. Radioactive bands migrating above MAGs represented less than 5% of products and were not identified. B, Quantification of MAG products from GPAT8 assays by autoradiography. The values represent means ± range of two independent enzyme preparations.

that GPAT6 is essential for the accumulation of C16 cutin monomers (Li-Beisson et al., 2009). When wheat germ-expressed GPAT6 was assayed with unmodified fatty acid, ω-OHFA, or DCA acyl-CoAs of chain length C16 to C24, substrates with either ω-functional group had a 4- to 11-fold higher activity compared with the corresponding unmodified acyl-CoAs (Fig. 3). Furthermore, GPAT6 had a clear chain length specificity. Activity with all of the C16 and C18 substrates was severalfold higher than with the corresponding acyl-CoAs of longer chain length (C20 or longer). In Arabidopsis flower cutin, 10,16-diOH C16:0-FA is the dominant monomer, whereas 16-OH C16:0-FA is a comparatively minor component (Li-Beisson et al., 2009). However, GPAT6 activity was higher with 16-OH C16:0-CoA than with 10,16-diOH C16:0-CoA (Fig. 3). To examine further

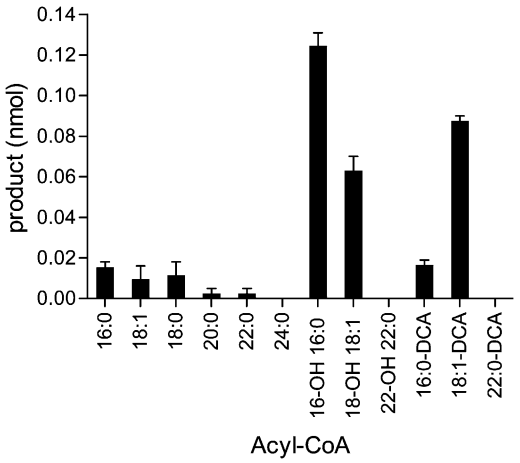

Figure 2. Substrate specificity of GPAT8. Wheat germ translation reaction expressing GPAT8 was used as the enzyme source. GPAT assays were conducted with different acyl-CoA species as acyl donors and [^{14}C]G3P as the acyl acceptor. Products (nmol) from vector control were subtracted from those of GPAT8 reactions. The values represent means ± range of two independent enzyme preparations.

whether GPAT6 displays acyl selectivity between 16-OH C16:0-CoA and 10,16-diOH C16:0-CoA, GPAT6 was incubated with equimolar mixtures of these two substrates at 10, 20, and 30 μM total acyl-CoA concentrations. In agreement with single substrate results, at each concentration GPAT6 exhibited fatty acid selectivity for 16-OH C16:0-CoA (Fig. 4A), producing 3- to 6-fold more product with the ω-hydroxy substrate than the dihydroxy substrate (Fig. 4B). To test if a mid-chain hydroxyl group increases acyl transfer activity compared with unmodified acyl-CoA, ricinoleoyl-CoA (12-OH C18:1-CoA) was synthesized and assayed with either GPAT6 or GPAT8. Almost no MAG formation was observed for either enzyme, indicating that mid-chain hydroxylation alone is not a positive determinant of activity (Supplemental Fig. S2).

Suberin-Associated GPAT5 Is an Acyltransferase with Broad Acyl-CoA Specificity

Very-long-chain (C20 or longer) fatty acids and their ω-oxidized derivatives are common aliphatic constituents of suberin. Arabidopsis GPAT5 is required for root and seed coat suberin biosynthesis, with *gpat5* mutants showing large reductions in C22:0- and C24:0-FA, ω-OHFA, and DCA monomers in seed coat suberin (Beisson et al., 2007). We previously demonstrated that GPAT5 is a *sn*-2-specific acyltransferase, but in contrast to GPAT4, -6, and -8, GPAT5 does not possess phosphatase activity; therefore, *sn*-2 LPA rather than *sn*-2 MAG is the major product (Yang et al., 2010). Acyl-CoA specificity of the GPAT5 enzyme was tested with ω-oxidized and unmodified acyl-CoAs with chain lengths from C16 to C24. The specificity of GPAT5 for acyl-CoA substrates is clearly distinct from GPAT4, -6, and -8 in two ways (Fig. 5). First, GPAT5 exhibited much broader chain length specificity. It was most active with acyl-CoA substrates of C22 chain length, but activity with other saturated substrates ranging from C16 to C24 differed only 40% to 45% compared with C22. Second, with longer chain length substrates, the enzyme did not discriminate between the oxidation states of acyl-CoAs (C22:0 normal FA/ω-OHFA/DCA). At C16 chain length, GPAT5 showed highest activity toward the unsubstituted acyl-CoA, reduced activity toward ω-OHFA-CoA, and lowest activity toward DCA-CoA. Activities with C18:1-FA, 18-OH C18:1-FA, and C18:1-DCA acyl-CoAs were among the lowest, suggesting discrimination against unsaturated substrates. In general terms, compared with GPAT4, -6, and -8, GPAT5 can accept a much wider range of acyl chain lengths, has a strong discrimination against cis-unsaturation and ω-oxidized C16 substrates, but does not discriminate strongly between oxidized and nonoxidized acyl-CoA substrates of longer chain lengths.

GPAT7 Likely Functions in Suberin Synthesis

Sequence analysis of the eight-member Arabidopsis GPAT family indicates that GPAT7 is most closely related to GPAT5 (Beisson et al., 2007; 88% similar and 81% identical amino acid sequences), and these two GPATs constitute a distinct clade of the gene family tree. We overexpressed GPAT7 in Arabidopsis, and this resulted in the production of very-long-chain *sn*-1/3- and *sn*-2 MAGs together with C22:0 and C24:0 free fatty acids in seed and stem waxes (Fig. 6). This phenotype is similar to

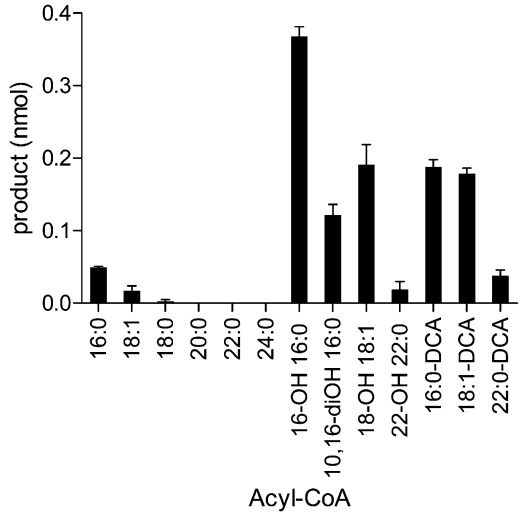

Figure 3. Substrate specificity of GPAT6. Wheat germ translation reaction expressing GPAT6 was used as the enzyme source. GPAT assays were conducted with acyl-CoA species shown as acyl donors and [^{14}C]G3P as the acyl acceptor. Products (nmol) from vector control were subtracted from those of GPAT6 reactions. The values represent means ± range of two independent enzyme preparations.

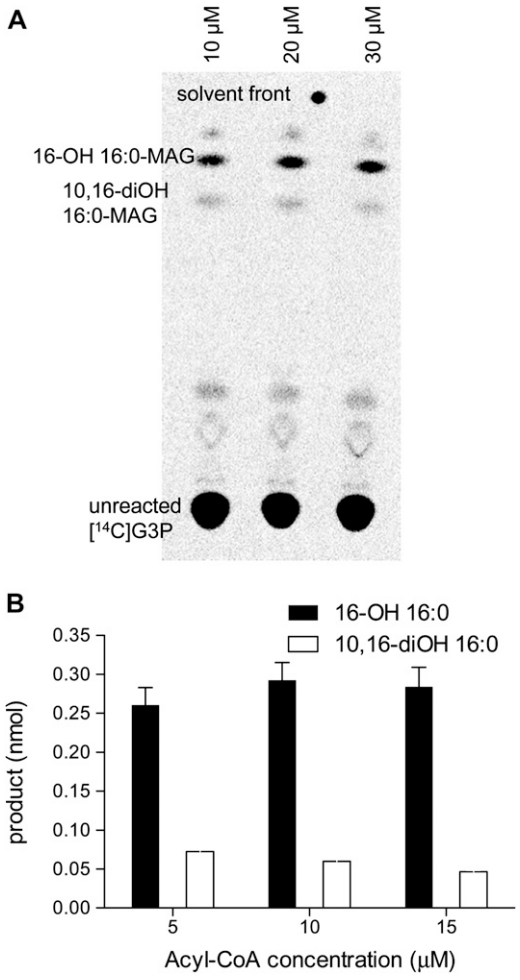

Figure 4. Fatty acid selectivity of GPAT6. Wheat germ translation reaction expressing GPAT6 was used as the enzyme source. GPAT assays were conducted with equimolar mixtures of 16-OH C16:0-CoA and 10,16-diOH C16:0-CoA species as acyl donors and [^{14}C]G3P as the acyl acceptor. After assay, the quenched reaction mixture was directly applied to a TLC plate (K6) and developed with chloroform:methanol:acetic acid:water (52:15:10:3.5). A, Radio-TLC image of product distribution. The large spot at the origin is unreacted [^{14}C]G3P. Radioactive bands below MAG were present in vector controls and represent impurities in the [^{14}C]G3P. Radioactive bands migrating above MAG represented less than 10% of products and were not identified. B, Quantification of the GPAT6 MAG product. The values represent means ± range of two independent enzyme preparations.

that found for GPAT5 ectopic expression (Li et al., 2007b) and suggests that GPAT7 acyl substrate specificity is similar to GPAT5. Suberin production in aerial tissues is a characteristic wounding response (Kolattukudy, 2001), and our data indicate that GPAT7 may participate in such a response. Indeed, promoter-GPAT7-GUS lines indicated that GPAT7 expression was strongly induced by wounding of leaf tissue (Fig. 7, A–C). In addition, compared with the wild type, the *gpat7* mutant did not develop resistance to toluidine blue staining at wound sites (Fig. 7, D–F). Taken together, the close sequence similarity to GPAT5, the production of soluble suberin-like precursors by overexpression lines, and the wound-induced expression all suggest that GPAT7 is a second member of the GPAT family that is involved in suberin synthesis. However, this hypothesis is tentative because leaf polyester analysis did not reveal changes of the composition in *gpat7* mutants (Supplemental Fig. S3), suggesting that GPAT7 may play a more specialized role in wounding or only in specific cell types.

GPAT1 Possesses *sn*-2 Acyltransferase But Not Phosphatase Activity

GPAT1 to -3 represent a distinct clade from the GPAT4/6/8 and GPAT5/7 clades in the GPAT family of Arabidopsis (Fig. 8). Because of the clear involvement of GPAT4 to -8 with cutin and suberin, we examined the polymeric lipids of *gpat1* but observed no clear chemical phenotype in mutant leaves, seeds, or flowers (Supplemental Fig. S4). In a previous characterization of Arabidopsis GPATs, GPAT1 was active with unsubstituted acyl-CoAs (C16:0, C16:1, C18:0, C18:1, and C20:1) whereas activity could not be detected for GPAT2 and -3 (Zheng et al., 2003). ω-oxidized acyl-CoAs typical of cutin and suberin were not tested. Because of the *sn*-2 regiospecificity of Arabidopsis GPAT4, -5, -6, and -8 and the bifunctional acyltransferase/phosphatase activity of GPAT4, -6, and -8, we reexamined and extended the analysis of activity and substrate specificity of Arabidopsis GPAT1 to -3 with a range of substrates from C16 to C24. As shown in Figure 9A, GPAT1 activity was highest with C20:0-CoA and 10-fold above C16:0 or C18:1 substrates. GPAT1 was also able to use C22:0 DCA-CoA with an equal preference to C22:0-CoA, indicating that GPAT1 is able to accept ω-oxidized acyl-CoAs, as we observed for GPAT4, -5, -6, and -8. We could not

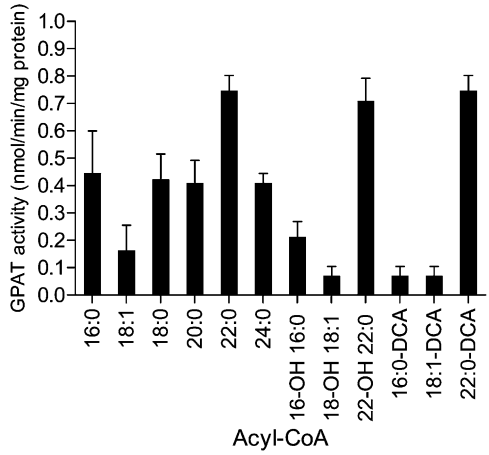

Figure 5. Substrate specificity of GPAT5. Microsomes from the yeast *gat1*Δ strain expressing GPAT5 were used as the enzyme source. GPAT assays were conducted with acyl-CoA species shown as acyl donors and [^{14}C]G3P as the acyl acceptor. GPAT activities from vector control were subtracted from those of GPAT5 reactions. The values represent means ± SD of three independent enzyme preparations.

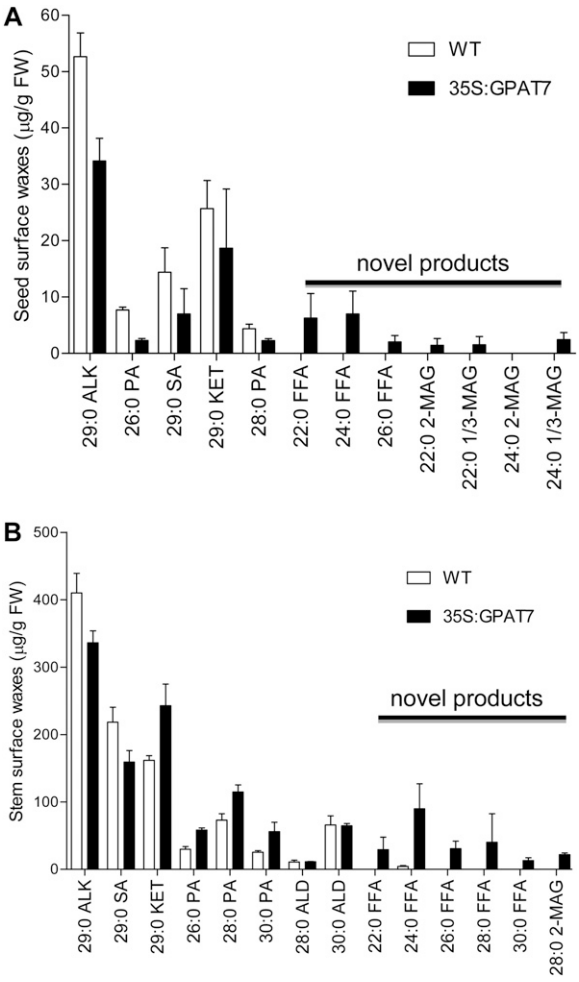

Figure 6. GPAT7 overexpression produces MAGs and free fatty acids in soluble chloroform-extractable surface lipids of the seeds (A) and stems (B). Three independent lines are averaged for the 35S:GPAT7 overexpressors, and error bars represent SD. ALD, Aldehyde; ALK, alkane; FFA, free fatty acid; FW, fresh weight; KET, ketone; PA, primary alcohol; SA, secondary alcohol; WT, wild type.

detect activity of GPAT2 and GPAT3 with either unmodified or ω-oxidized substrates in either the yeast or wheat germ expression system. It is possible that an appropriate substrate has not yet been tested or that a component is missing from the assay. We also analyzed *gpat2* and *gpat3* mutants, and neither displayed any obvious phenotypes or changes in their polymeric lipids of flowers, leaves, or in the seeds (Supplemental Fig. S4). Even though GPAT2 and -3 have lost the key amino acids in their phosphatase domain, they retain their HXXXXD and CPEGT conserved acyltransferase domain motifs and so may be expected to be active acyltransferases.

LPAs rather than MAGs were the products of the GPAT1 reaction. Therefore, GPAT1 does not possess the phosphatase activity characteristic of GPAT4, -6, and -8. GPAT1 has only one change in its key amino acid residues in the phosphatase domain. The first Asp in motif III has been replaced with Ser. In GPAT6, when the equivalent residue was mutated from Asp to Lys, this was sufficient to ablate all phosphatase activity (Yang et al., 2010). To determine if GPAT1 catalyzes the transfer of the acyl-CoA to the *sn*-1 or *sn*-2 position of G3P, the phosphate group of the product was removed by hydrolysis with alkaline phosphatase to produce MAG. The regiospecificity of the resultant MAG products was determined by immediate application of hydrolysis products to borate-TLC to resolve *sn*-1 from *sn*-2 isomers. The observed products of C18:0-CoA and C20:0-CoA reactions were only *sn*-2 MAGs. For C22:0-DCA-CoA substrate, the major MAG product also comigrated with C22:0-DCA *sn*-2 MAG standard generated by GPAT5 assay (Fig. 9B). Therefore, these and previous results indicate that enzymes from all three clades of the GPAT family are *sn*-2 acyltransferases.

DISCUSSION

sn-2 Regiospecificity Is a Distinctive Property of the Land-Plant-Specific Lineage of GPATs

The acyl-CoA:*sn*-glycerol-3-phosphate 1-*O*-acyltransferase (EC 2.3.1.15) that carries out the first acylation of G3P to produce *sn*-1 LPA has been extensively characterized in membrane and storage lipid synthesis of plants, animals, and prokaryotes (Murata and Tasaka, 1997; Zheng and Zou, 2001; Gimeno and Cao, 2008; Zhang and Rock, 2008; Wendel et al., 2009; Chen et al., 2011a). The accumulation of *sn*-2 MAGs in surface lipids of Arabidopsis by ectopic expression of GPAT5 (Li et al., 2007b) opened the question of the regiospecificity of GPATs that are involved in plant polyester synthesis. We recently demonstrated that GPAT5 is indeed a *sn*-2 acyltransferase. Furthermore, GPAT4 and GPAT6 are also *sn*-2 acyltransferases with an additional phosphatase activity (Yang et al., 2010). These results provide, to our knowledge, the first evidence that the initial steps of cutin and suberin synthesis differ fundamentally from the de novo biosynthesis of membrane and storage glycerolipids. In this study, we have further demonstrated that cutin-associated GPAT8 is also a bifunctional *sn*-2 acyltransferase/phosphatase and that GPAT1 from the third, less-characterized clade possesses *sn*-2 regiospecificity as well. Thus, all five of the GPATs probed for their enzymatic regiospecificity are *sn*-2 specific. These represent all three clades. In addition, we can infer at least substantial *sn*-2 specificity for GPAT7 from the occurrence of *sn*-2 MAG on ectopic expression (Fig. 6). This only leaves GPAT2 and -3 from the eight genes with undetermined regioselectivity. However, based on structural modeling (Supplemental Fig. S5) and sequence similarities in the active site, it appears likely that GPAT2 and -3 are also *sn*-2 specific. To differentiate between GPAT enzymes with different regiospecificity, a new EC number (EC 2.3.1.198) has been assigned to the *sn*-2-specific GPAT reaction by the

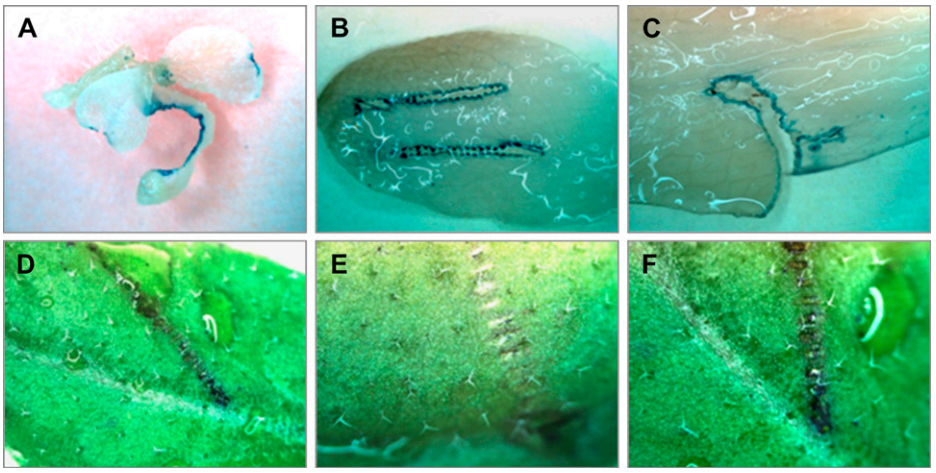

Figure 7. GPAT7 expression is induced by wounding, and *gpat7* mutants are impaired in wound response. A to C, GPAT7 promoter::GUS responds to wounding. Strong GUS staining was detected only in wounded regions of leaves. D to F, Compared with wild-type leaves, the *gpat7-1* mutant fails to exclude toluidine blue after wounding. Rosette leaves (6 weeks old) were wounded with tweezers and kept in standard growth conditions for 48 h. Leaves were then detached from plants and stained with toluidine blue (0.05%) to test tissue-sealing capacities. D, Freshly wounded wild-type leaves are permeable to toluidine blue. E, After 48 h, wild-type leaves are impermeable to toluidine blue, indicating suberin-type wound-sealing response. F, After 48 h, *gpat7-1* leaves are still permeable to toluidine blue. Similar observations were also made for other *gpat7* alleles (data not shown). Plant tissue images presented in this study were taken with a light microscope (Leica MZ 12.5) coupled with a digital camera.

Enzyme Nomenclature Committee of the International Union of Biochemistry and Molecular Biology. To provide clarity in this discussion, we will often refer to these enzymes collectively as *sn*-2-GPATs to distinguish them from GPATs with *sn*-1 regiospecificity. And, as discussed in detail below, they can also be defined as "land-plant-specific GPATs" because close homologs first appear with the primitive mosses and are not found in animals, fungi, or microorganisms (Yang et al., 2010).

The underlying reasons for the distinctive *sn*-2 regiospecificity remain to be determined. The *sn*-2 LPA or MAG products are thermodynamically less stable (by about 4 kJ mol^{-1}) than *sn*-1 isoforms. Thus, acyl migration between the two positions produces products at a ratio of approximately 4:1 in favor of a primary position over the secondary position. Does biosynthesis with *sn*-2 regiospecificity impart to cutin and suberin a uniquely advantageous polymer property? Or does *sn*-2 provide a "recognition signal" for targeting polymer precursors to specific transport and assembly processes? Or, more simply, does the difference from the *sn*-1 acylation pathway for membrane lipids allow selective metabolism of similar LPA intermediates destined for different pathways? These unknowns await further biochemical and cellular evidence.

Insight into the Cutin/Suberin Biosynthetic Pathway: Evidence That Acyl Oxidation Precedes Acyl Transfer to Glycerol

An unanswered question in cutin and suberin biosynthesis is the exact biosynthetic pathway to these polyesters. Even this question is clearly hindered by lack of a definitive view of polyester assembly and structure. Nevertheless, largely through the study of mutants, members of the activating enzymes of the LACS family, the fatty acid P450 oxidases, and GPATs have all been shown clearly to be required for cutin and suberin biosynthesis, controlling both composition and the total amount of polyester accumulation (Beisson et al., 2012). LACS2 is required for optimum cutin synthesis (Bessire et al., 2007) and is active with both normal and ω-OHFA (Schnurr et al., 2004). In vitro characterization of CYP86 P450s to date has demonstrated ω-hydroxylation activity with free fatty acids (FFAs; Benveniste et al., 2006; Rupasinghe et al., 2007; Pinot and Beisson, 2011) and also with acyl-CoAs (Han et al., 2010). However, whether the ordering of the acyl oxidation and the acyl transfer reactions occurs as pathway A [FFA (*LACS*, *P450*)→oxidized acyl-CoA (*GPAT*)→oxidized *sn*-2 MAG] or pathway B [FFA (*LACS*)→acyl-CoA (*GPAT*)→*sn*-2 MAG (*P450*)→oxidized *sn*-2 MAG] remains undetermined (Pollard et al., 2008), with the exception that the acyl-CoA synthetase must precede *sn*-2-GPAT to provide acyl-CoA substrates for acyl transfer reactions.

The enzymology of *sn*-2-GPATs with unmodified and ω-oxidized acyl-CoA substrates is instructive in addressing this unknown in the biosynthetic pathway. The two Arabidopsis GPATs (GPAT4 and -8) that are involved in leaf and stem cutin biosynthesis exhibited 10-fold or higher activity toward ω-oxidized acyl-CoA substrates than the unsubstituted acyl-CoAs. Similarly, recombinant GPAT6, required for flower cutin synthesis, exhibited the following acyl specificity for C16:0 chain length (Fig. 3): 16-OH C16:0 > C16:0-DCA > 10,16-diOH C16:0 > C16:0. Previously, based on in planta evidence, a biosynthetic route for Arabidopsis

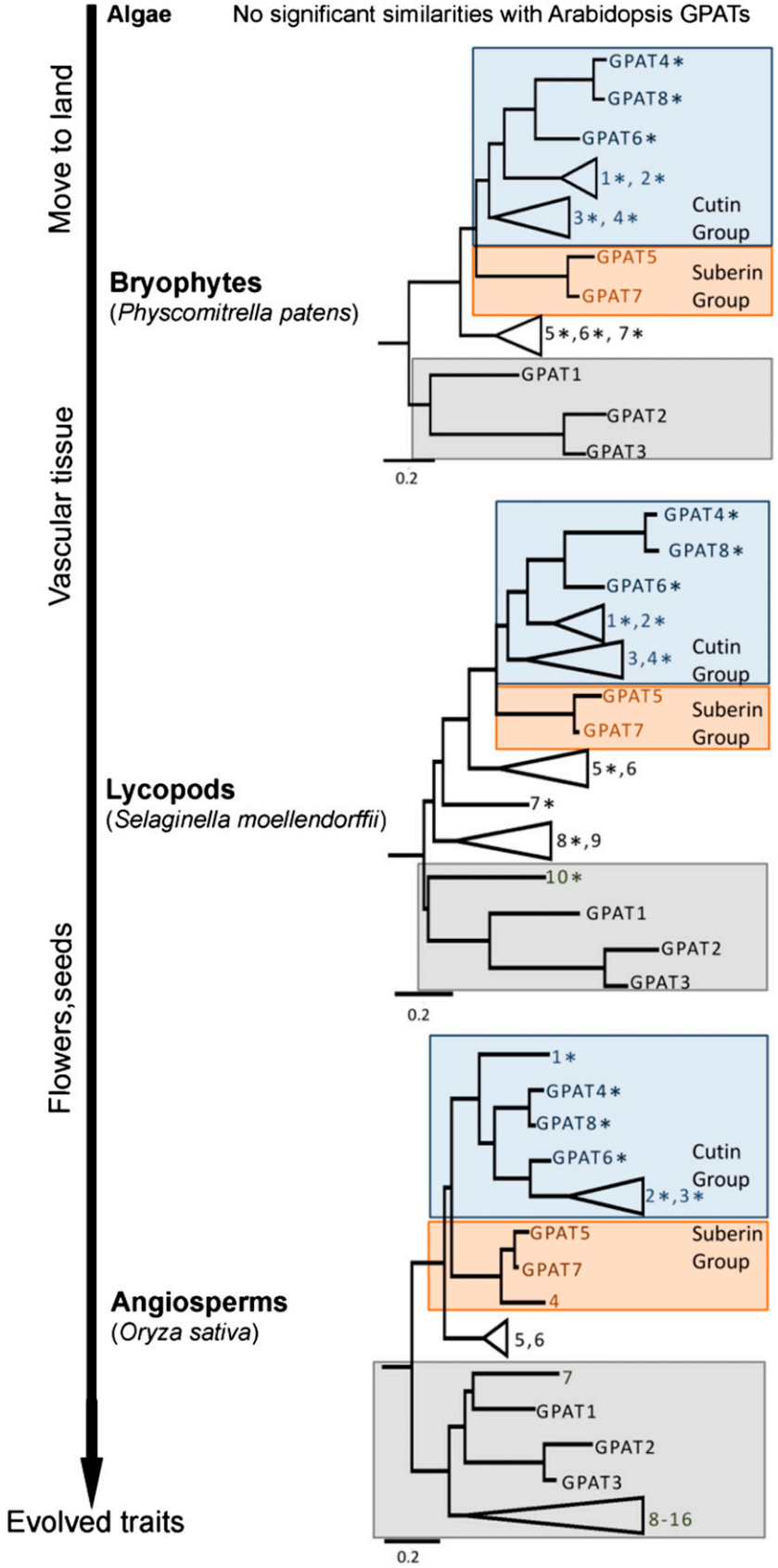

Figure 8. Phylogenies of Arabidopsis GPATs from green plants. Each phylogeny illustrates the phylogenetic relationships between the eight members of the Arabidopsis GPAT family and their homologs in angiosperms (rice), early vascular plants (*S. moellendorffii*), and early land plants (*P. patens*). In each phylogeny, the Arabidopsis GPATs are identified as GPAT1 to GPAT8, while the genes from the other species are identified by numbers (for annotations, see "Materials and Methods"). The asterisk beside some genes indicates that it has a phosphatase domain, as identified by InterProScan (http://www.ebi.ac.uk/Tools/pfa/iprscan/). The three clades of *sn*-2-GPATs are highlighted in different colors, representing the GPAT4/6/8 clade (blue), the GPAT5/7 clade (orange), and the GPAT1/2/3 clade (gray). The scale to the left represents the traits that are thought to have evolved in the representative species.

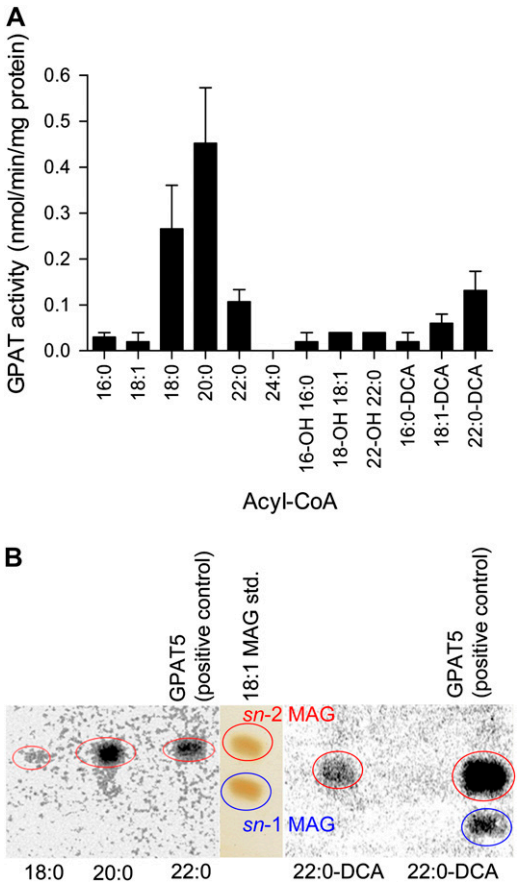

Figure 9. Substrate specificity and regiospecificity of GPAT1. A, Substrate specificity of GPAT1. Microsomes from the yeast *gat1*Δ strain expressing GPAT1 were used as the enzyme source. GPAT assays were conducted using the acyl-CoA species shown and [^{14}C]G3P as substrates. GPAT activities from vector control were subtracted from those of GPAT1 reactions. The values represent means ± SD of three independent enzyme preparations. B, GPAT1 is a *sn*-2 acyltransferase. The reaction mixture containing C18:0-LPA, C20:0-LPA, or C22:0-FA-LPA was treated with 1 unit of alkaline phosphatase and analyzed by borate-TLC by comparison with C22:0 or C22:0-DCA *sn*-2 MAG generated from the alkaline phosphatase treatment of GPAT5 assay.

C16:0-derived flower cutin monomers was proposed (Li-Beisson et al., 2009) in which 16-OH C16:0-FA can lead to the production of either C16:0-DCA or 10,16-diOH C16:0-FA. The production of C16:0-DCA requires as yet unidentified oxidases and/or dehydrogenases, while 10,16-diOH C16:0-FA is produced in vitro by CYP77A6 from 16-OH C16:0-FA (Li-Beisson et al., 2009). However, the reaction order of GPAT6 and ω-oxidation reactions was unresolved. If GPAT6 preceded all the oxidation reactions (i.e. if acylglycerols were the in vivo substrates for all the oxidation reactions), C16:0-CoA would be expected to be the best or at least a strong in vitro substrate for GPAT6. However, the opposite is observed. If GPAT6 functioned at the branch point, acylating glycerol with 16-OH C16:0-FA to provide *sn*-2 MAG as substrate, would C16:0-DCA and 10,16-diOH C16:0-FA still be active substrates for GPAT6? If they were not substrates, the subsequent oxidations would be downstream of GPAT6. But as they are good substrates (Fig. 3), the situation remains ambiguous. If mid-chain hydroxylation (and DCA formation) occurs preferentially to GPAT6 acylation, the fact that this dominant cutin monomer 10,16-diOH C16:0-FA is not the preferred acyl substrate for GPAT6 will have to be taken into account in any eventual model for biosynthesis.

This leaves the most likely scenario for GPAT6, as with GPAT4 and -8, to function after the ω-oxidation reaction and probably after subsequent oxidations. Together, these substrate specificity data strongly support the pathway of oxidations first, GPAT second and thus expand our understanding of the cutin and suberin biosynthetic pathways. Nevertheless, since 2-MAGs have not been tested as additional substrates for P450s, we cannot rule out the possibility that oxidation reactions could also occur after the acyl transfer step. Unlike GPAT4/6/8, GPAT5 can utilize both normal and ω-oxidized fatty acids approximately equally (Fig. 5). However, as described in the next section, analysis of *gpat5* and other mutants can provide further evidence for ω-hydroxylation preceding acyl transfer.

sn-2-GPAT Acyl Specificity as a Determinant of Cutin/Suberin Composition

The in vivo products of acyltransferase reactions depend on enzyme specificity and also on the substrate pools available to the enzyme. Comparison of the in vitro enzyme specificities determined in this study with the in vivo consequences of their disruption or overexpression can provide an indication of the contributions of these alternatives. The fact that we do not know how the expression of any one gene may coregulate other genes in the pathway, nor the extent to which metabolic feedback inhibition may control flux, and substrate pool size and composition, prevents full interpretation. As we postulate that oxidation precedes acyl transfer, the feedback inhibition may act at either of these steps, but most logically at the former.

Of the cutin-associated acyltransferases, Arabidopsis GPAT4 and GPAT8 are essential for leaf and stem cutin synthesis (Li et al., 2007a). In our substrate specificity study, both GPAT4 and -8 are severalfold more active toward most ω-oxidized acyl-CoA substrates than the unmodified acyl-CoAs and exhibit 5- to 60-fold greater activity for C16:0 and C18:1 acyl groups compared with C20:0, C22:0, or C24:0. In agreement with the in vitro data, double knockouts of these enzymes (*gpat4/gpat8*) are reduced overall 60% to 70% in C16 and C18 cutin monomers, with the greatest reduction observed in C18:2-DCA. Furthermore, overexpression of either GPAT4 or GPAT8 markedly increases C16/C18 ω-OHFA and DCA compared with the nonoxidized monomers (Li et al., 2007a). In

agreement with the results in Arabidopsis, increases or decreases of C16/C18 leaf cutin monomers are observed after ectopic expression of a GPAT4/8 homolog from *Echium pitardii* in tobacco (Mañas-Fernández et al., 2010) or by silencing of GPAT4 homologs in *Brassica napus* (Chen et al., 2011b). Thus, for most monomers, the in vivo data coincide with in vitro enzyme specificity data.

Unlike the C18 monomers that predominate in stems and leaves, Arabidopsis flower cutin monomers are largely of C16 chain length (approximately 70%). GPAT6 is the most highly expressed acyltransferase in flowers. As with GPAT4 and -8, recombinant GPAT6 activity is substantially higher with oxidized acyl-CoAs (16-OH C16:0, C16:0-DCA, and 10,16-diOH C16:0) than with unmodified C16:0-CoA (Fig. 3). The *gpat6* mutants display 80% to 95% reductions in these C16 monomers with little change in C18 monomers or in unmodified C16:0. When GPAT6 is overexpressed in stems, these C16 monomers are all increased in unison (3- to 6-fold) with little change in C18 unsaturated monomers (Li-Beisson et al., 2009). Because C16 monomers are minor components of stem cutin (which is dominated by C18:2-DCA), this specific increase of oxidized C16 monomers illustrates control by GPAT6 specificity over cutin composition. GPAT6 also has strong activity toward C18:1 ω-oxidized monomers (Fig. 3) that were not altered by overexpression and thus implies control by both enzyme specificity and substrate supply over the final composition.

The most notable phenotype of Arabidopsis g*pat5* mutants is the more than 80% reduction in C22:0 and C24:0 ω-OHFA and DCA aliphatic monomers and the corresponding nonoxidized acyl chains of seed coat suberin (Beisson et al., 2007). There is a similar reduction of both normal and ω-oxidized fatty acid monomers in root suberin of *gpat5* mutants. These seed coat and root data suggest that GPAT5 can utilize either very-long-chain ω-oxidized or normal fatty acids for polyester synthesis. This is exactly what we observe in vitro (Fig. 5) for C22:0 normal, ω-OH, and DCA substrates. Coexpression of GPAT5 with CYP86A1 (Li et al., 2007a) or CYP86B1 (Molina et al., 2009) produces C16 to C24 ω-oxidized monomers in stem cutin. This is consistent with the wide chain length specificity of GPAT5 determined in vitro, spanning at least C16 to C24 chain lengths (Fig. 5). The appearance of monomers with C20 and C22 chain lengths in stems clearly reflects the broad GPAT5 specificity, because no changes were observed with overexpression of CYP86A1 or CYP86B1 alone, and reinforces the determination of GPAT enzyme specificity to cutin composition. The accumulation of very-long-chain MAGs (C22–C30) in the surface waxes of GPAT5 overexpressors (Li et al., 2007b) shows that GPAT5 acyl chain length in vivo extends to at least C30. In addition, roots of 3-week-old *gpat5* Arabidopsis seedlings show large reductions in C16:0 and C18:1 ω-OHFAs but not DCAs (Beisson et al., 2007). The synthesis of these C16:0 and C18:1 ω-OHFAs and DCAs requires the ω-hydroxylase CYP86A1 (Li et al., 2007a; Höfer et al., 2008). As the accumulation of ω-OHFA requires GPAT5 but the synthesis of DCA, which goes through the same P450, does not, then a simple explanation is that GPAT5 is required for the incorporation of ω-OHFA into cutin but not for the ω-hydroxylation itself. A second argument for placing ω-hydroxylation before GPAT5 acyl transfer comes from the observation that the seed suberin monomer 1,22-docosane-diol requires CYP86B1 (Molina et al., 2009) for its synthesis but not GPAT5 (Beisson et al., 2007; Molina et al., 2008). As its synthesis presumably proceeds via the action of an acyl-CoA reductase on 22-OH C22:0-CoA, the inference here again is that glycerol acylation is not required for ω-hydroxylation.

Summarizing across two distinctive cutin types and suberin, there is an overall correspondence between in vivo monomer compositions in the wild type and mutants and in vitro GPAT acyl specificity data. The acyl specificities also highlight an important distinction between cutin- and suberin-associated GPATs: that is, the broad chain length acyl specificity of the latter. The C16/C18 specificity of the cutin-associated GPATs allows a clear metabolic separation, and presumably independent control, between cutin and very-long-chain cuticular wax biosynthesis. This complete separation is not possible with the suberin-associated GPATs. Ectopic expression of GPAT5 changes cuticular wax composition (Li et al., 2007b). GPAT knockouts severely limit cutin monomer accumulation, while enhanced expression of GPAT4, -6, or -8 alone or GPAT5 in combination with CYP86A1 (Li et al., 2007a) or CYP86B1 (Molina et al., 2009) genes can increase monomer yield 2-fold or more. This suggests that GPATs have at least partial control on flux through the pathway, possibly via the relief of feedback inhibition on the preceding ω-oxidases. GPAT specificity together with substrate supply control monomer composition. However, the high expression correlation between specific sets of GPAT and P450 genes (Pollard et al., 2008; Beisson et al., 2012) and the requirement for GPAT5 and its cognate P450s to generate additional C16 to C22 monomers in stem cutin show that we should really consider acyl specificity as a coevolved attribute.

Placing GPATs in their broader biosynthetic perspective is difficult. The extent to which particular cutins and suberins are extended aliphatic polyesters or more complex heteropolymers is unknown. MAGs may be exported monomers (synthons) for extracellular polymerization by transacylases, such as proposed for the Gly-Asp-Ser-Leu (GDSL) lipase CD1 in C16-rich tomato fruit cutin (Yeats et al., 2012). However, intracellular oligomerization may occur. MAGs might be initiators for further intracellular polymerization, or the addition of glycerol may be an intracellular oligomerization terminator. Such alternatives will require the identification of the requisite intracellular enzymes and further characterization of GPATs with a series of estolide acyl-CoAs.

sn-2 Regiospecific GPAT Evolution and Divergence

Phylogenetic relationships can provide information on gene function (Eisen, 1998). Almost every enzyme of primary glycerolipid metabolism in plants has strong homologs in bacteria, fungi, or animals. In contrast, searches against prokaryote and nonphotosynthetic eukaryotic sequences, and of the fully sequenced *Chlamydomonas reinhardtii*, *Volvox carteri*, and other algal genomes, do not identify any GPATs with significant similarities (BLASTX $E < 10^{-5}$) to the *sn*-2-GPATs found in land plants. Thus, the *sn*-2-GPAT family studied here is clearly a land-plant-specific lineage and implies that it evolved in land plants to provide pathways for functions not present in other organisms. The family of *sn*-2-GPAT enzymes is distinct in other fundamental aspects from all other characterized GPAT enzymes that are *sn*-1 *O*-acyltransferases. First, in addition to *sn*-2 regiospecificity, GPAT4, -6, and -8 are bifunctional acyltransferase/phosphatases, resulting in *sn*-2 MAG products. Second, *sn*-2-GPAT expression is predominantly epidermal (Suh et al., 2005). Third, GPAT4 has been observed in Arabidopsis plasma membranes by proteomic analysis (Mitra et al., 2009), whereas a putative *sn*-1-GPAT but not *sn*-2-GPAT homologs have been identified by proteomics of purified castor endoplasmic reticulum membranes (Brown et al., 2011). Fourth, based on analysis of mutants of all eight Arabidopsis members, and *E. pitardii* GPAT4/8 homologs (Mañas-Fernández et al., 2010), no members of this land-plant-specific GPAT family have been shown to be directly involved in the production of membrane or storage lipids. Minor changes in the glycerolipid composition of mutants that have been reported (Zheng et al., 2003; Li et al., 2012) are likely to be secondary consequences of disturbances of the extracellular lipids. Finally, the gene family encoding *sn*-2-GPAT enzymes is larger than *sn*-1-specific GPAT families. Of the over 30 available land-plant genomes, all possess at least six genes with strong similarity to the Arabidopsis *sn*-2-GPATs. In contrast, the *sn*-1-specific GPAT families of other eukaryotes are smaller. For example, yeast and mammals possess two and four genes, respectively.

The expansion and divergence of the *sn*-2-GPAT family into three distinct conserved clades (Fig. 8) is associated with key stages in the morphological and functional evolution of land plants and also coincides with the loss of phosphatase activity in GPATs. The most ancient extant land-plant lineage, Bryophyta (nonvascular), evolved from algae more than 425 million years ago (Sanderson, 2003; Lewis and McCourt, 2004). Cuticle evolution would be critical during this landmark transition from aquatic to terrestrial habitats (Riederer, 2006). Indeed, there is fossil evidence (Taylor, 1988) and both chemical and/or anatomical evidence of a cuticle in the earliest nonvascular land plants, including *Sphagnum* species, *Physcomitrella patens* (mosses; Cook and Graham, 1998), and *Asterella* species (liverworts; Caldicott and Eglinton, 1976). This early association to the *sn*-2-GPAT family is clearly observed at the molecular genetic level by the appearance of strong homologs ($E < 10^{-100}$) to *sn*-2-specific GPATs in the genomes of *P. patens* and the lycopod *Selaginella moellendorffii*. It is notable that all these ancient lineages possess genes that specifically cluster within the Arabidopsis GPAT4/6/8 clade, and of these, all possess conserved phosphatase active site residues (Yang et al., 2010). This implies that the GPAT4/6/8 clade is the most ancient and was involved in the assembly of cutin or cutin-like polymers in the first land plants. Furthermore, all other fully sequenced angiosperms, and also gymnosperms, possess genes that cluster within the cutin-associated GPAT4/6/8 clade, indicating conservation of this clade throughout the evolution of higher plants.

The divergence of the land-plant-specific GPAT family to form the GPAT5/7 clade is associated with (1) the evolution of tracheophytes (i.e. vascular plants), (2) the loss of phosphatase active site residues, and (3) likely the evolution of suberin polymers. In Arabidopsis, GPAT5 is required for the production of suberin in the endodermis and also the seed coat outer integument (Beisson et al., 2007). The suberized endodermis is believed to be ubiquitous in all vascular plants and may have evolved from polyesters that existed in the stems of the common ancestor to all tracheophytes (Boyce, 2005). Sequences that fall within the GPAT5/7 clade are conserved in all fully sequenced tracheophytes, with the exception of the lycopod *S. moellendorffii*, which is a sister group to all other tracheophytes (Banks, 2009) and may have independently evolved to synthesize polyesters specific to tracheophytes.

Sequences of the GPAT1 to -3 clade are more divergent compared with the GPAT4/6/8 and GPAT5/7 clades. All available fully sequenced angiosperms possess more than one gene in this clade, and the clade appears to be present only in vascular plants, as no homologs appear in *P. patens* and only one in *S. moellendorffii* (Fig. 8). Functionally, within the Arabidopsis GPAT1 to -3 clade, we were able to detect acyltransferase activity with GPAT1. This activity is clearly *sn*-2 specific and, like GPAT5, active with both ω-oxidized and unmodified acyl-CoA (Fig. 9). In Arabidopsis, GPAT1 is clearly associated with flower development, as its expression is enriched in flowers and siliques and *gpat1* mutant plants exhibit abnormal tapetum development and reduced pollen production (Zheng et al., 2003). Moreover, a *gpat1/gpat6* double mutant displays more severe phenotypes than either single mutant and is male sterile (Li et al., 2012). The specific biochemical reaction catalyzed by GPAT1 in vivo remains elusive. However, a biological function of GPAT1 in flowers likely extends to monocots because the expression of its closest rice (*Oryza sativa*) homolog (Os01g44069) is enriched in stigmas (Rice eFP browser). The function of the GPAT2 and -3 members of this branch remains unknown. Acyltransferase activity could not be demonstrated for

GPAT2 and GPAT3 with either ω-oxidized or unmodified acyl-CoAs, as observed with unmodified acyl-CoAs by Zheng et al. (2003). It is possible that an appropriate substrate or cofactor has not yet been tested. In contrast to GPAT1, the tissue-level expression patterns of Arabidopsis GPAT2 and -3 are broader than GPAT1 (Beisson et al., 2007; Winter et al., 2007). We also analyzed T-DNA insertion mutants for GPAT2 and GPAT3, and none display any obvious growth or polyester composition phenotypes (Supplemental Fig. S4). Thus, the likely production of *sn*-2 glycerolipids by GPAT2 and -3 and their role in higher plants remain unknown.

Evolution of *sn*-2-Specific GPAT through Gene Fusion and the Role of Phosphatase Domain Architecture

Gene fusion usually leads to the physical linkage of proteins that have different functions but participate in a common metabolic pathway or biological process. The two-domain structure of the *sn*-2-GPAT family almost certainly evolved from an ancient gene fusion event that occurred in a common ancestor to land plants. When analyzed individually, neither the N-terminal phosphatase domain nor the C-terminal acyltransferase domain from any land-plant *sn*-2-GPAT exhibits strong similarity ($E < 10^{-6}$) to any acyltransferase or phosphatase enzyme in nonphotosynthetic organisms or algae. Thus, an ancestral progenitor for either domain is not clear. In the N-terminal phosphatase domain, the first Asp in motif I, the first Lys in motif III, and the first Asp in motif III are essential for the phosphatase activity of GPAT6 (Yang et al., 2010). In land plants, the bifunctional GPAT is likely the ancestral enzyme activity, because all GPATs in *P. patens* have the active site residues required for phosphatase activity (Yang et al., 2010). Furthermore, in all fully sequenced angiosperms, all genes within the cutin-associated GPAT4/6/8 clade retain critical phosphatase residues, while all genes in the later-evolving GPAT5/7 and GPAT1/2/3 clades have lost conserved residues (Fig. 8). Thus, as noted above, the loss of phosphatase activity is clearly correlated with the functional divergence of *sn*-2-GPATs and expansion of the family. Nevertheless, it is clear that MAG synthesis via a phosphatase activity is required and could be provided by another protein that preexisted or coevolved to compensate for the loss of phosphatase activity. Alternatively, although the loss of the key active site residues of the phosphatase domain is evident in early vascular plants, the tertiary structure of the N-terminal 250 amino acids has been preserved throughout the evolution of angiosperms (Yang et al., 2010; Supplemental Fig. S5). The conservation of this structure may imply additional functions, perhaps relevant to acyltransferase activity, or protein-protein interactions. In this regard, Gidda et al. (2009, 2011) concluded that both the N- and C-termini face the cytosol, potentially allowing the two domains to interact. Conservation of structure associated with an inactive catalytic domain has also been observed for protein Tyr phosphatase (Tonks, 2006). Furthermore, it is known that nonactive sites can sometimes be restored by the addition of ligands. One such example is the rescue of mutant protein Tyr kinase activity in living cells by the addition of imidazole (Qiao et al., 2006). Although speculative, perhaps in planta the phosphatase activity of *sn*-2-GPATs can be restored through interactions with a ligand or other protein. Collectively, these features imply that the N-terminal architecture surrounding the "phosphatase" domain likely remained critical for the function of all clades within the *sn*-2-GPAT family.

MATERIALS AND METHODS

Materials

The haploid gene disruption strain YKR067w::kanMX4 (*BY4742; Matα; his3Δ1; leu2Δ0; lys2Δ0; ura3Δ0; YKR067w::kanMX4*) was purchased from EUROSCARF. [^{14}C(U)]Glycerol-L-3-phosphate was from American Radiolabeled Chemicals. C16:0-, C18:1-, C18:0-, and C20:0-CoAs were purchased from Sigma-Aldrich, and C22:0- and C24:0-CoAs were from Avanti Polar Lipids. The synthesis of acyl-CoAs with ω-oxidized functional groups is described below. Borate-TLC plates (Partisil K6 silica gel 60 Å, 250 μm; Whatman) were prepared by dipping in 10% boric acid in methanol and activation at 110°C for 30 min immediately before use. Unless stated otherwise, all other reagents were from Sigma-Aldrich.

Cloning and Heterologous Expression of GPATs in Yeast *gat1Δ* Strain

The previous constructs GPAT4/pYES2-CT and GPAT5/pYES-DEST52 (Yang et al., 2010) were used in this study. For GPAT1, plasmid containing its coding sequence was obtained from the Arabidopsis Biological Resource Center (ABRC) at Ohio State University. The gene was amplified by PCR with primers GPAT1-cF and GPAT1-cR (Supplemental Table S2). The amplified PCR products were ligated into the yeast (*Saccharomyces cerevisiae*) expression vector pYES2/CT (Invitrogen) and verified by sequencing. Transformation and heterologous expression of the genes in the yeast GPAT-deficient mutant *gat1Δ* strain, and further isolation of the microsomes necessary for assaying acyltransferase activity, were performed as described previously (Yang et al., 2010). Protein concentrations of the microsomes were determined via the Pierce bicinchoninic acid protein assay (Thermo Scientific) using fatty acid-free bovine serum albumin as the standard.

Cloning and Expression of GPAT6 and -8 in a Wheat Germ Cell-Free Translation System

Plasmid containing the coding sequence for GPAT8 was obtained from the ABRC. The coding sequence of GPAT8 was amplified by PCR with primers GPAT8-cF and GPAT8-cR (Supplemental Table S2). The amplified PCR products were ligated directly into RTS pIVEX wheat germ His-6-tag vector pIVEX 1.3WG (Roche Applied Science) and verified by sequencing. The previously made construct GPAT6/pIVEX1.4WG (Yang et al., 2010) was also used in this study. Translation of GPAT6 and GPAT8 from constructs GPAT6/pIVEX1.4WG and GPAT8/pIVEX1.3WG was achieved by using RTS 100 Wheat Germ CECF Kit (5 PRIME) according to the manufacturer's instructions. Liposomes (10 mg mL^{-1}) were prepared from acetone-washed soybean lethicin (L-α-phosphatidylcholine) and added at 60 μg per reaction. The reaction mixtures containing translated proteins were stored at −80°C before direct use in the assays.

Synthesis and Identification of ω-Oxidized Acyl-CoAs

10,16-diOH C16:0-FA was isolated and purified from extractive-free tomato (*Solanum lycopersicum*) peel powders through transmethylation (Molina

et al., 2006), preparative TLC (Croteau and Fagerson, 1972), and saponification of the purified fatty acid methyl ester. 18-OH C18:1-FA was purified from tobacco (*Nicotiana tabacum*) stigma lipids (Matsuzaki et al., 1983), while 22-OH C22:0-FA was isolated from extractive-free cork (*Quercus suber*) powders. Greater than 95% purity for each was achieved by transmethylation, sequential preparative TLC (K6 silica with development with hexane:diethyl ether solvent mixtures, 65:35 for 18-OH C18:1-FA, 1:1 for 22-OH C22:0-FA), C18 reverse-phase HPLC (semipreparative column 218TP510, 10 mm × 250 mm, isocratic elution with 55% acetonitrile/water for 18-OH C18:1-FA, 70% acetonitrile/water for 22-OH C22:0-FA), and the saponification process. C18:1-DCA (a gift from Cognis) and C22:0-DCA (Sigma-Aldrich) were purified to more than 95% before use. The above purified fatty acids together with 16-OH C16:0-FA (98%; Sigma-Aldrich) and C16:0-DCA (more than 98%; Sigma-Aldrich) were used for acyl-CoA synthesis using a carbonyldiimidazole-based method (Kawaguchi et al., 1981). The structures of ω-oxidized acyl-CoAs (C16:0, C18:1, and C22:0) were confirmed by ESI-MS and ESI-MS/MS (Supplemental Table S1) as detailed previously (Yang et al., 2010). DCA possesses two carboxyl groups; thus, the production of DCA bis-CoA thioester is possible. Bis-CoA thioester was not detected as products by TLC or ESI-MS/MS.

GPAT Activity Assay

GPAT activity was determined by quantifying the amount of [^{14}C(U)]G3P substrate incorporated into products (LPA, phosphatidic acid, or MAG; Yang et al., 2010). GPAT assay was performed in a 30-μL reaction mixture containing 37.5 mM Tris-HCl (pH 7.5), 0.5 mM G3P (with 0.1 μCi of [^{14}C]G3P), 45 μM acyl-CoA, 4 mM NaF, 2 mM $MgCl_2$, 1 mM dithiothreitol, and 0.1% bovine serum albumin (fatty acid free) at room temperature for 10 min. Either wheat germ translation reaction mixture (2 μL) or yeast microsomes (20 μg) was the enzyme source. Immediately following the assay, the entire reaction was spotted onto a K6 TLC plate, developed with $CHCl_3$:CH_3OH:HAc:H_2O (85:15:10:3.5, 68:15:10:3.5, or 52:15:10:3.5). The yeast *gat1*Δ strain containing empty vector pYES-DEST52 or pYES2-CT was used as GPAT5 and GPAT1 to -4 assay controls, respectively. Wheat germ expressing empty vector pIVEX1.4 WG or pIVEX1.3 WG was used as GPAT6 and GPAT8 assay controls, respectively. Radiolabeled products were identified by comigration with standards and quantified by autoradiography on an Instant Imager (Packard) or Personal Molecular Imager (Bio-Rad). Some details of the enzyme assays themselves are presented in Supplemental Figure S6.

Regiospecificity of GPAT1 and GPAT8

Positional analysis of LPA from GPAT1 assay was performed immediately after the GPAT assay. Briefly, four separate GPAT assays were combined, added to 0.1 M borate buffer (pH 7.5, 1 mL) and 0.1 M Tris-HCl (pH 7.5, 970 μL), and treated with 1 unit of *Escherichia coli* alkaline phosphatase with shaking for 30 min at room temperature. The lipids were extracted by diethyl ether and evaporated to dryness. The products were dissolved in 100 μL of chloroform and separated on a borate-TLC plate developed in chloroform: acetone (1:1). We used a borate-TLC plate because it allows for clear separation of α-MAG (*sn*-1/*sn*-3 MAG) from β-MAG (*sn*-2 MAG) with minimal acyl migration. Positive identification of the regiospecificity of MAGs was achieved by comparing with the R_f values of *sn*-2 MAGs obtained from the simultaneous hydrolysis of *sn*-2 LPA produced from GPAT5 assay. The regiospecificity of MAGs from GPAT8 assay was analyzed by spotting the entire GPAT reaction on a borate-TLC plate. *sn*-2 MAGs produced by GPAT8 were positively identified by comigration with ω-OH or DCA *sn*-2 MAGs produced from the GPAT6 assay.

Phylogenetic Analysis of Land-Plant-Specific GPATs

Homologs of each member of the Arabidopsis (*Arabidopsis thaliana*) *sn*-2-GPAT family were identified by BLASTP searches with data sets from www.phytozome.org. Only those sequences with an E-value less than 10^{-50} were considered as members of the family. In each tree, for gene sequences other than Arabidopsis GPATs, the number at each node tip, or numbers beside the collapsed braches, corresponds to the following sequences, using the nomenclature found at www.phytozome.org. *Physcomitrella patens*: (1) Pp1s134_51V6.1; (2) Pp1s9_453V6.1; (3) Pp1s117_135V6.1; (4) Pp1s42_150V6.1; (5) Pp1s117_125V6.1; (6) Pp1s72_49V6.1; (7) Pp1s281_69V6.1. *Selaginella moellendorffii*: (1) Sm_80614; (2) Sm_170163; (3) Sm_405228; (4) Sm_118115; (5) Sm_63752; (6) Sm_405007; (7) Sm_80075; (8) Sm_90219; (9) Sm_233008; (10) Sm_164779. Rice (*Oryza sativa*): (1) Os2g02340.1; (2) Os01g63580.1; (3) Os05g37600.1; (4) Os05g38350.1; (5) Os03g52570.1; (6) Os10g27330.1; (7) Os01g44069.1; (8) Os11g45400.1; (9) Os12g37600.1; (10) Os01g14900.1; (11) Os05g20100.1; (12) Os01g19390.1; (13) Os10g41070.1; (14) Os08g03700.1; (15) Os03g61720.1; (16) Os01g22560.1. Multiple alignments and the phylogenetic trees were generated using bioinformatic tools available at www.phylogeny.fr, using the default settings (MUSCLE 3.7 was used for multiple alignment, Gblocks 0.91b was used for alignment refinement, and PhyML 3.0 was used to generate the phylogenies; trees were created using Fig tree 1.3.1. [http://tree.bio.ed.ac.uk/]). The bar on each phylogeny indicates the branch length that corresponds to the number of substitutions per position.

Plant Materials and Growth Conditions

Arabidopsis ecotype Columbia was used throughout this study. The plants were grown in a controlled chamber (at 21°C–22°C, 40%–60% relative humidity, and a 16/8-h photoperiod at 80–100 μmol m^{-2} s^{-1} provided by fluorescent bulbs). Transgenic plants were first selected on Murashige and Skoog agar plates supplemented with 50 μg mL^{-1} kanamycin before being transferred to soil for further analyses.

Isolation of Homozygous Mutants for *gpat1*, *gpat2*, *gpat3*, and *gpat7*

All mutants used in this study were ordered from the ABRC with the SALK collection. Combinations of gene-specific primers were used together with the T-DNA left border primer LBa1 for selection of homozygous plants. Homozygous lines were obtained for GPAT1, GPAT2, GPAT3, and GPAT7 from SALK_052352 (*gpat1*), SALK_118230 (*gpat2*), SALK_028578 (*gpat3*), SALK_063846 (*gpat7-1*), SALK_006822 (*gpat7-2*), and SALK_064514 (*gpat7-3*). Detailed information on primers used in this study is shown in Supplemental Table S2.

GPAT7 Overexpression, Wound Response, and Promoter-GUS Fusion Analyses

For GPAT7 overexpression, the genomic DNA (including one intron) was cloned and inserted into binary vector pBI121 as an *Xba*I-*Sac*I fragment and introduced into *Agrobacterium tumefaciens* strain C58C1 for Arabidopsis flower dip transformation (Clough and Bent, 1998). Cloning primer sequences are shown in Supplemental Table S2. For wound-response analysis, Arabidopsis rosette leaves (6 weeks old) were wounded with tweezers and kept in standard growth conditions for 48 h. Leaves were then detached from plants and stained with toluidine blue (0.05%) to test tissue-sealing capacities. Plant tissue images presented in this study were taken with a light microscope (Leica MZ 12.5) coupled with a digital camera. To examine GPAT7 (At5g06090) expression, promoter sequences (1,619 bp) upstream of the starting ATG codon were obtained from the AGRIS Web site (http://arabidopsis.med.ohio-state.edu/) and cloned into the binary vector pBI101 in fusion with the GUS protein; the resulting construct was named pBI101:GPAT7.

Lipid Analyses

Stem and seed waxes were analyzed according to a previous cuticular wax analysis protocol (Li et al., 2007b).

For polyester analyses, depending on the tissues used, polyester monomers were analyzed following previously published protocols (Beisson et al., 2007; Molina et al., 2008).

The accession numbers of Arabidopsis GPAT1 to -8 are as follows: GPAT1, At1g06520; GPAT2, At1g02390; GPAT3, At4g01950; GPAT4, At1g01610; GPAT5, At3g11430; GPAT6, At2g38110; GPAT7, At5g06090; and GPAT8, At4g00400.

Supplemental Data

The following materials are available in the online version of this article.

Supplemental Figure S1. Substrate specificity of GPAT4.

Supplemental Figure S2. GPAT6 and GPAT8 activity with ricinoleoyl-CoA.

Supplemental Figure S3. Leaf polyester analysis of *gpat7*-1 mutant before and after wounding.

Supplemental Figure S4. Polyester analyses of *gpat1*, *gpat2*, and *gpat3* mutants.

Supplemental Figure S5. Models for N-terminal domains of Arabidopsis GPAT1, -4, and -7.

Supplemental Figure S6. GPAT assay-substrate concentration dependence and comments on glycerol production.

Supplemental Table S1. Identification of ω-oxidized acyl-CoAs by ESI-MS/MS.

Supplemental Table S2. Primer sequences.

ACKNOWLEDGMENTS

We thank Prof. Michael Feig for protein N-terminal structure modeling and Dr. Dylan Kosma for critical reading of the manuscript. We thank the Michigan State University Research Technology Support Facility and Mass Spectrometry Facility.

Received June 14, 2012; accepted August 3, 2012; published August 3, 2012.

LITERATURE CITED

Banks JA (2009) Selaginella and 400 million years of separation. Annu Rev Plant Biol **60:** 223–238

Beisson F, Li Y, Bonaventure G, Pollard M, Ohlrogge JB (2007) The acyltransferase GPAT5 is required for the synthesis of suberin in seed coat and root of *Arabidopsis*. Plant Cell **19:** 351–368

Beisson F, Li-Beisson Y, Pollard M (2012) Solving the puzzles of cutin and suberin polymer biosynthesis. Curr Opin Plant Biol **15:** 329–337

Benveniste I, Saito T, Wang Y, Kandel S, Huang HW, Pinot F, Kahn RA, Salaun JP, Shimoji M (2006) Evolutionary relationship and substrate specificity of *Arabidopsis thaliana* fatty acid omega-hydroxylase. Plant Sci **170:** 326–338

Bernards M (2002) Demystifying suberin. Can J Bot **80:** 227–240

Bessire M, Chassot C, Jacquat AC, Humphry M, Borel S, Petétot JMC, Métraux JP, Nawrath C (2007) A permeable cuticle in Arabidopsis leads to a strong resistance to *Botrytis cinerea*. EMBO J **26:** 2158–2168

Boyce K (2005) The evolutionary history of roots and leaves. *In* M Holbrook, M Zwieniecki, eds, Vascular Transport in Plants. Elsevier Academic Press, Burlington, MA, pp 479–499

Brown AP, Kroon JTM, Topping JF, Robson JL, Simon WJ, Slabas AR (2011) Components of complex lipid biosynthetic pathways in developing castor (*Ricinus communis*) seeds identified by MudPIT analysis of enriched endoplasmic reticulum. J Proteome Res **10:** 3565–3577

Caldicott AB, Eglinton G (1976) Gas chromatographic-mass spectrometric studies of long-chain hydroxy-acids.7. Cutin acids from Bryophytes: omega-1 hydroxy alkanoic acid in 2 liverwort species. Phytochemistry **15:** 1139–1143

Chen X, Snyder CL, Truksa M, Shah S, Weselake RJ (2011a) sn-Glycerol-3-phosphate acyltransferases in plants. Plant Signal Behav **6:** 1695–1699

Chen X, Truksa M, Snyder CL, El-Mezawy A, Shah S, Weselake RJ (2011b) Three homologous genes encoding *sn*-glycerol-3-phosphate acyltransferase 4 exhibit different expression patterns and functional divergence in *Brassica napus*. Plant Physiol **155:** 851–865

Clough SJ, Bent AF (1998) Floral dip: a simplified method for Agrobacterium-mediated transformation of Arabidopsis thaliana. Plant J **16:** 735–743

Cook ME, Graham LE (1998) Structural similarities between surface layers of selected charophycean algae and bryophytes and the cuticles of vascular plants. Int J Plant Sci **159:** 780–787

Croteau R, Fagerson IS (1972) Constituent cutin acids of cranbury cuticle. Phytochemistry **11:** 353–363

Eisen JA (1998) Phylogenomics: improving functional predictions for uncharacterized genes by evolutionary analysis. Genome Res **8:** 163–167

Gidda SK, Shockey JM, Falcone M, Kim PK, Rothstein SJ, Andrews DW, Dyer JM, Mullen RT (2011) Hydrophobic-domain-dependent protein-protein interactions mediate the localization of GPAT enzymes to ER subdomains. Traffic **12:** 452–472

Gidda SK, Shockey JM, Rothstein SJ, Dyer JM, Mullen RT (2009) *Arabidopsis thaliana* GPAT8 and GPAT9 are localized to the ER and possess distinct ER retrieval signals: functional divergence of the dilysine ER retrieval motif in plant cells. Plant Physiol Biochem **47:** 867–879

Gimeno RE, Cao J (2008) Thematic review series: glycerolipids. Mammalian glycerol-3-phosphate acyltransferases: new genes for an old activity. J Lipid Res **49:** 2079–2088

Graça J, Lamosa P (2010) Linear and branched poly(omega-hydroxyacid) esters in plant cutins. J Agric Food Chem **58:** 9666–9674

Graça J, Santos S (2007) Suberin: a biopolyester of plants' skin. Macromol Biosci **7:** 128–135

Han J, Clement JM, Li J, King A, Ng S, Jaworski JG (2010) The cytochrome P450 CYP86A22 is a fatty acyl-CoA omega-hydroxylase essential for estolide synthesis in the stigma of *Petunia hybrida*. J Biol Chem **285:** 3986–3996

Höfer R, Briesen I, Beck M, Pinot F, Schreiber L, Franke R (2008) The Arabidopsis cytochrome P450 *CYP86A1* encodes a fatty acid ω-hydroxylase involved in suberin monomer biosynthesis. J Exp Bot **59:** 2347–2360

Kawaguchi A, Yoshimura T, Okuda S (1981) A new method for the preparation of acyl-CoA thioesters. J Biochem **89:** 337–339

Kolattukudy PE (2001) Polyesters in higher plants. Adv Biochem Eng Biotechnol **71:** 1–49

Lewis LA, McCourt RM (2004) Green algae and the origin of land plants. Am J Bot **91:** 1535–1556

Li XC, Zhu J, Yang J, Zhang GR, Xing WF, Zhang S, Yang ZN (2012) Glycerol-3-phosphate acyltransferase 6 (GPAT6) is important for tapetum development in Arabidopsis and plays multiple roles in plant fertility. Mol Plant **5:** 131–142

Li Y, Beisson F, Koo AJ, Molina I, Pollard M, Ohlrogge JB (2007a) Identification of acyltransferases required for cutin biosynthesis and production of cutin with suberin-like monomers. Proc Natl Acad Sci USA **104:** 18339–18344

Li Y, Beisson F, Ohlrogge JB, Pollard M (2007b) Monoacylglycerols are components of root waxes and can be produced in the aerial cuticle by ectopic expression of a suberin-associated acyltransferase. Plant Physiol **144:** 1267–1277

Li-Beisson Y, Pollard M, Sauveplane V, Pinot F, Ohlrogge JB, Beisson F (2009) Nanoridges that characterize the surface morphology of flowers require the synthesis of cutin polyester. Proc Natl Acad Sci USA **106:** 22008–22013

Mañas-Fernández A, Li-Beisson Y, Alonso DL, García-Maroto F (2010) Cloning and molecular characterization of a glycerol-3-phosphate O-acyltransferase (GPAT) gene from *Echium* (Boraginaceae) involved in the biosynthesis of cutin polyesters. Planta **232:** 987–997

Matsuzaki T, Koiwai A, Kawashima N (1983) Changes in stigma-specific lipids of tobacco plant during flower development. Plant Cell Physiol **24:** 207–213

Mitra SK, Walters BT, Clouse SD, Goshe MB (2009) An efficient organic solvent based extraction method for the proteomic analysis of Arabidopsis plasma membranes. J Proteome Res **8:** 2752–2767

Molina I, Bonaventure G, Ohlrogge J, Pollard M (2006) The lipid polyester composition of *Arabidopsis thaliana* and *Brassica napus* seeds. Phytochemistry **67:** 2597–2610

Molina I, Li-Beisson Y, Beisson F, Ohlrogge JB, Pollard M (2009) Identification of an Arabidopsis feruloyl-coenzyme A transferase required for suberin synthesis. Plant Physiol **151:** 1317–1328

Molina I, Ohlrogge JB, Pollard M (2008) Deposition and localization of lipid polyester in developing seeds of *Brassica napus* and *Arabidopsis thaliana*. Plant J **53:** 437–449

Murata N, Tasaka Y (1997) Glycerol-3-phosphate acyltransferase in plants. Biochim Biophys Acta **1348:** 10–16

Nishida I, Tasaka Y, Shiraishi H, Murata N (1993) The gene and the RNA for the precursor to the plastid-located glycerol-3-phosphate acyltransferase of *Arabidopsis thaliana*. Plant Mol Biol **21:** 267–277

Pinot F, Beisson F (2011) Cytochrome P450 metabolizing fatty acids in plants: characterization and physiological roles. FEBS J **278:** 195–205

Pollard M, Beisson F, Li Y, Ohlrogge JB (2008) Building lipid barriers: biosynthesis of cutin and suberin. Trends Plant Sci **13:** 236–246

Qiao Y, Molina H, Pandey A, Zhang J, Cole PA (2006) Chemical rescue of a mutant enzyme in living cells. Science **311:** 1293–1297

Ranathunge K, Schreiber L, Franke R (2011) Suberin research in the genomics era: new interest for an old polymer. Plant Sci **180:** 399–413

Rensing SA, Lang D, Zimmer AD, Terry A, Salamov A, Shapiro H, Nishiyama T, Perroud PF, Lindquist EA, Kamisugi Y, et al (2008) The *Physcomitrella* genome reveals evolutionary insights into the conquest of land by plants. Science **319:** 64–69

Riederer M (2006) Introduction: biology of the plant cuticle. *In* M Riederer, C Muller, eds, Biology of the Plant Cuticle, Vol 23. Blackwell Publishing, Oxford, pp 1–10

Rupasinghe SG, Duan H, Schuler MA (2007) Molecular definitions of fatty acid hydroxylases in *Arabidopsis thaliana*. Proteins **68:** 279–293

Sanderson MJ (2003) Molecular data from 27 proteins do not support a Precambrian origin of land plants. Am J Bot **90:** 954–956

Schnurr J, Shockey J, Browse J (2004) The acyl-CoA synthetase encoded by *LACS2* is essential for normal cuticle development in *Arabidopsis*. Plant Cell **16:** 629–642

Schreiber L (2010) Transport barriers made of cutin, suberin and associated waxes. Trends Plant Sci **15:** 546–553

Suh MC, Samuels AL, Jetter R, Kunst L, Pollard M, Ohlrogge J, Beisson F (2005) Cuticular lipid composition, surface structure, and gene expression in Arabidopsis stem epidermis. Plant Physiol **139:** 1649–1665

Taylor TN (1988) The origin of land plants: some answers, more questions. Taxon **37:** 805–833

Tonks NK (2006) Protein tyrosine phosphatases: from genes, to function, to disease. Nat Rev Mol Cell Biol **7:** 833–846

Wendel AA, Lewin TM, Coleman RA (2009) Glycerol-3-phosphate acyltransferases: rate limiting enzymes of triacylglycerol biosynthesis. Biochim Biophys Acta **1791:** 501–506

Winter D, Vinegar B, Nahal H, Ammar R, Wilson GV, Provart NJ (2007) An "Electronic Fluorescent Pictograph" browser for exploring and analyzing large-scale biological data sets. PLoS ONE **2:** e718

Yang W, Pollard M, Li-Beisson Y, Beisson F, Feig M, Ohlrogge J (2010) A distinct type of glycerol-3-phosphate acyltransferase with *sn*-2 preference and phosphatase activity producing 2-monoacylglycerol. Proc Natl Acad Sci USA **107:** 12040–12045

Yeats TH, Martin LB, Viart HM, Isaacson T, He Y, Zhao L, Matas AJ, Buda GJ, Domozych DS, Clausen MH, et al (2012) The identification of cutin synthase: formation of the plant polyester cutin. Nat Chem Biol **8:** 609–611

Zhang YM, Rock CO (2008) Thematic review series: glycerolipids. Acyltransferases in bacterial glycerophospholipid synthesis. J Lipid Res **49:** 1867–1874

Zheng Z, Xia Q, Dauk M, Shen W, Selvaraj G, Zou J (2003) *Arabidopsis AtGPAT1*, a member of the membrane-bound glycerol-3-phosphate acyltransferase gene family, is essential for tapetum differentiation and male fertility. Plant Cell **15:** 1872–1887

Zheng Z, Zou J (2001) The initial step of the glycerolipid pathway: identification of glycerol 3-phosphate/dihydroxyacetone phosphate dual substrate acyltransferases in *Saccharomyces cerevisiae*. J Biol Chem **276:** 41710–41716

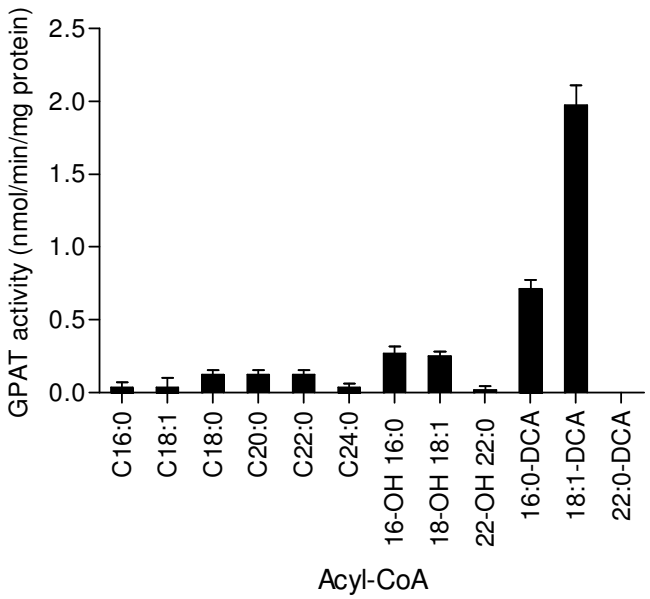

Supplemental Figure S1. Substrate specificity of GPAT4. Microsomes from the yeast *gat1*Δ strain expressing GPAT4 were used as the enzyme source. GPAT assays were conducted with different acyl-CoA species as acyl donors and [^{14}C]G3P as the acyl acceptor. GPAT activities from vector control were subtracted from those of GPAT4 reactions. The values represent the mean ± SD of three independent enzyme preparations.

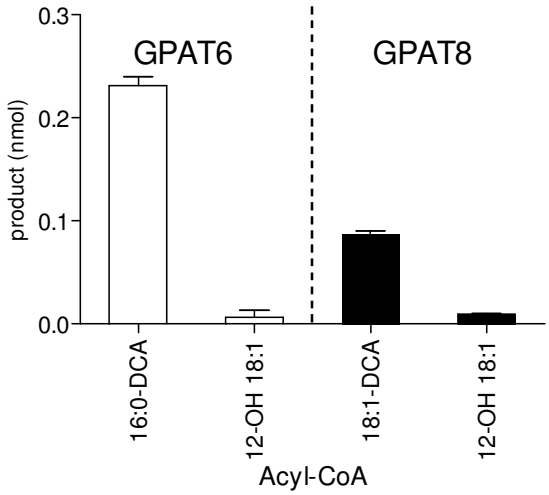

Supplemental Figure S2. GPAT6 and GPAT8 activity with ricinoleoyl-CoA. Wheat germ translation reactions expressing GPAT6 or GPAT8 were used as the enzyme source. GPAT assays were conducted with ricinoleoyl-CoA (i.e. 12-OH C18:1-CoA) as acyl donor and [^{14}C]G3P as the acyl acceptor. Assays with C16:0 DCA-CoA or C18:1 DCA-CoA were used as positive control*s* for GPAT6 and GPAT8, respectively. Values represent the mean ± range of two independent enzyme preparations.

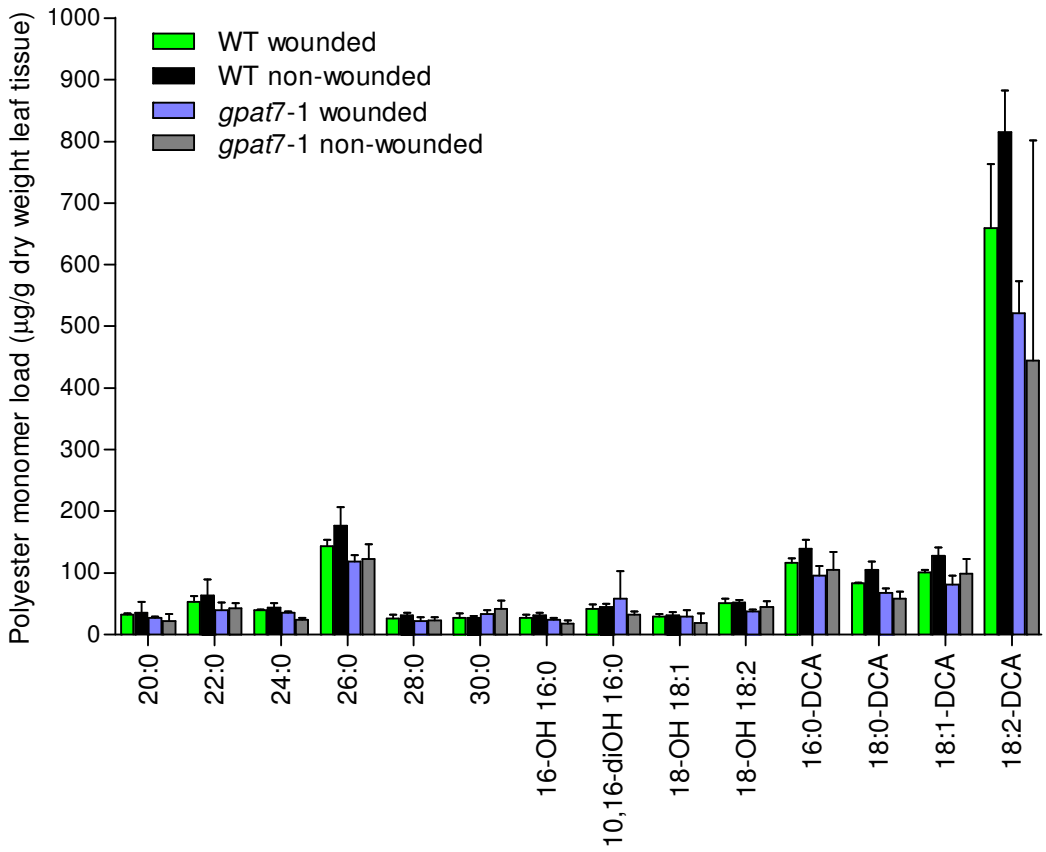

Supplemental Figure S3. Comparison of leaf polyester content and composition between WT and *gpat7-1* mutant, before and after wounding. Healthy rossette leaves (6-week-old) were wounded 5 times in each leaf with tweezers as shown in Figure 7. Leaf tissues were harvested for polyester analyses before and after wounding for 48 hours. Data are mean ± standard deviation (n=3).

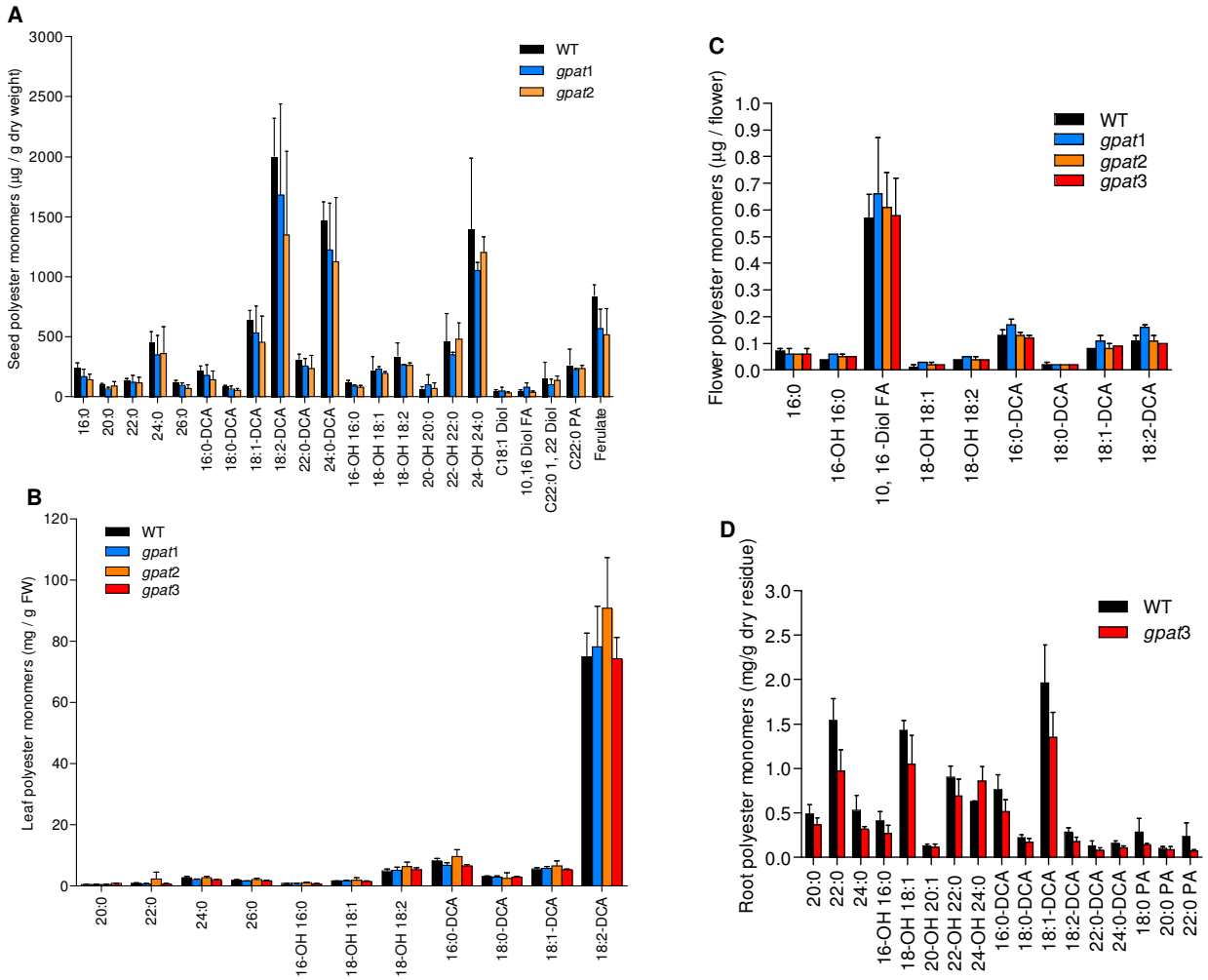

Supplemental Figure S4. Polyester monomer analyses for seed (A), leaf (B), flower (C) and root (D) of *gpat1, gpat2* and *gpat3* mutants. Data are mean ± standard deviation (n=3).

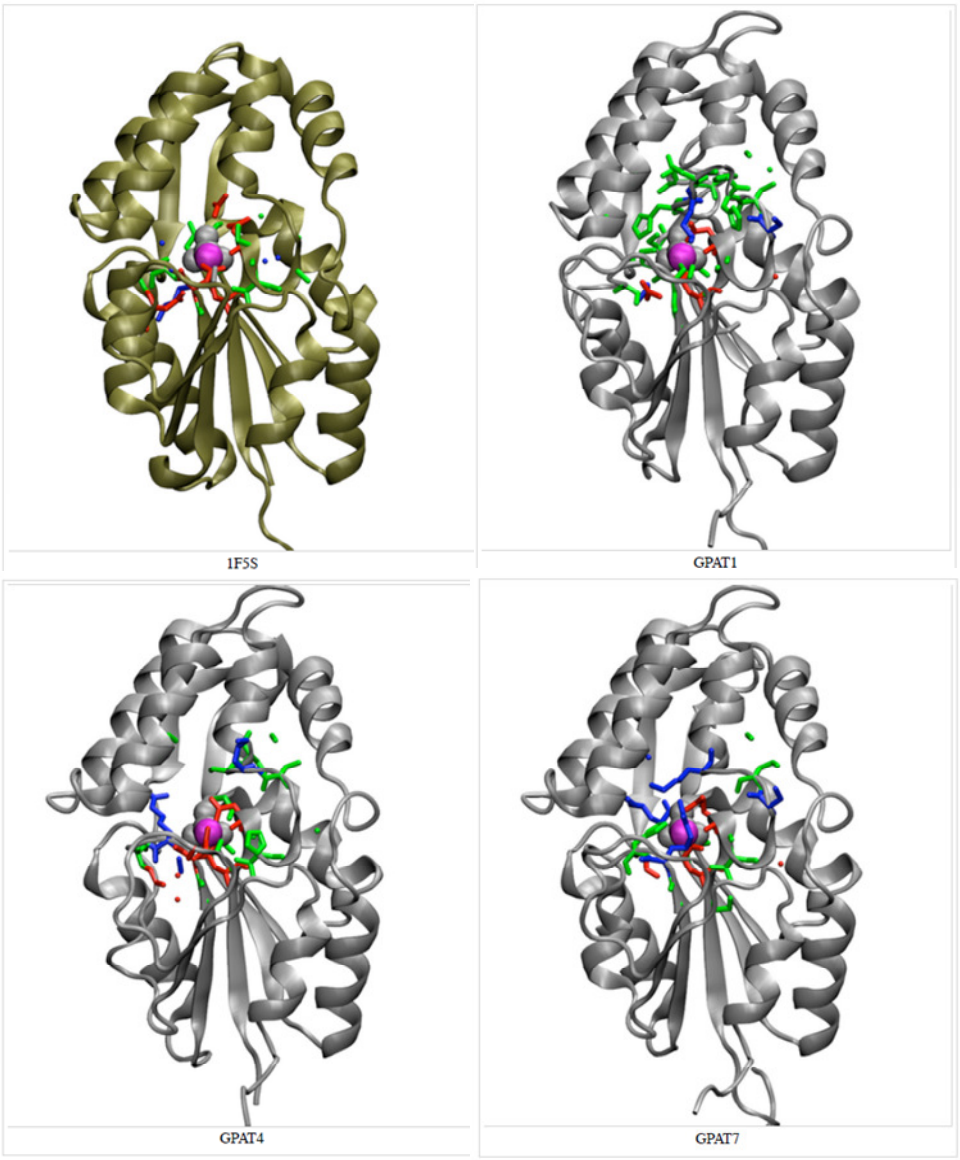

Supplemental Figure S5. Models for N-terminal Domains of AtGPAT1, 4 and 7 based on *Methanococcus jannaschii Phosphoserine* Phosphatase (PDB: 1F5S). The structures above were predicted based on the crystal structure of 1F5S. Active site residues in N-terminal domain of GPAT4 are shown in Yang et al (2010). The conserved acidic residues (red) interact with Mg^{2+} (purple) in the active site, which facilitates the phosphatase activity. Although some active site residues are changed in GPAT1 and GPAT7, the N-term tertiary structure remains conserved.

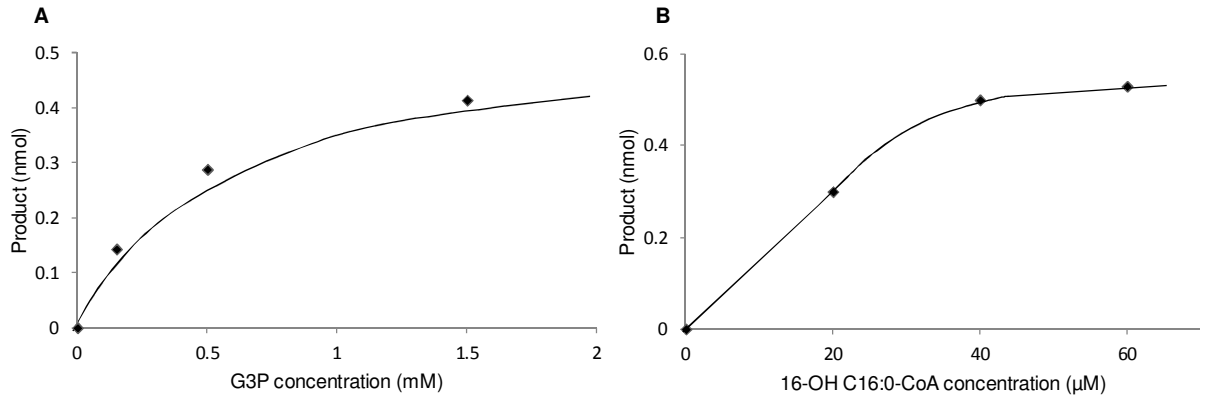

Supplemental Figure S6. GPAT Assay – Substrate concentration dependence and comments on glycerol production. Assays were in the linear range for product accumulation versus time and protein, as reported earlier (Yang et al., 2010). The yields from the ω-oxidized acyl-CoA syntheses were low (< 200 nmoles), preventing determination of acyl-CoA Km and Vmax values and other kinetic parameters for all substrates for the GPATs. Supplemental Figure S6A shows the G3P concentration curve for GPAT4 for yeast microsomes assayed with 45 μM C18:1 DCA-CoA. Averages for duplicate determinations are shown. The standard assay G3P concentration of 0.5 mM is just above its approximate Km value of 0.4 mM. Supplemental Figure S6B shows GPAT6 produced by the wheat germ translation reaction assayed with 16-OH C16:0-CoA (0, 20, 40 or 60 μM) and 0.5 mM G3P. The standard assay concentration of 45 μM is close to assay saturation for this substrate. However, as different acyl-CoAs have different critical micelle concentrations and can exhibit substrate inhibition in enzyme assays, this can only be taken as an approximation of substrate dependence for assays with other substrates.

Glycerol-3-phosphate acyltransferase activity was determined by quantifying the amount of [^{14}C]G3P substrate incorporated into LPA, PA or MAG products (Yang et al., 2010). However, we note that in the assay of GPAT4 and GPAT6 in the yeast system, [^{14}C]glycerol is also a co-product. More specifically, GPAT4 or GAPT6 assayed with C16 or C18:1 ω-OH acyl-CoA produced [^{14}C]glycerol as a major co-product along with LPA and MAG. Vector only control assays produced almost no [^{14}C]glycerol, nor did GPAT assayed without acyl-CoA substrate. In contrast, GPAT4 and 6 expressed in a wheat germ cell-free translation system produced little [^{14}C]glycerol, with MAG as the only major product. GPAT5 assayed with yeast microsomes does not exhibit this aberrant phosphatase to produce [^{14}C]glycerol, presumably because it has no active phosphatase domain. This side reaction is absent in the wheat germ system. The reasons for glycerol production from recombinant GPATs from yeast but not from wheat-germ remain obscure. The yeast microsomes may provide LPA phospholipase and/or MAG lipase activity. Or the activity may be a function of an altered GPAT enzyme in yeast when compared to wheat germ, which is hydrolyzing either G3P or acyl product. Therefore, Arabidopsis GPAT6 and GPAT8 were assayed in the wheat germ system, which provided simple MAG products. Since we were unable to obtain active GPAT4 by wheat-germ expression, this enzyme, and GPAT1 and 5 were characterized in the yeast system.

A

Acyl-CoA	$[M+H]^+$	[acyl pantetheine + H]$^+$
10,16-diOH 16:0	1038.3	531.3
16-OH 16:0	1022.4	515.3
16:0-DCA	1036.3	529.4
18-OH 18:1	1048.3	541.3
12-OH 18:1	1048.3	541.4
18:1-DCA	1062.4	555.4
22-OH 22:0	1106.5	599.5
22:0-DCA	1120.3	613.3

B

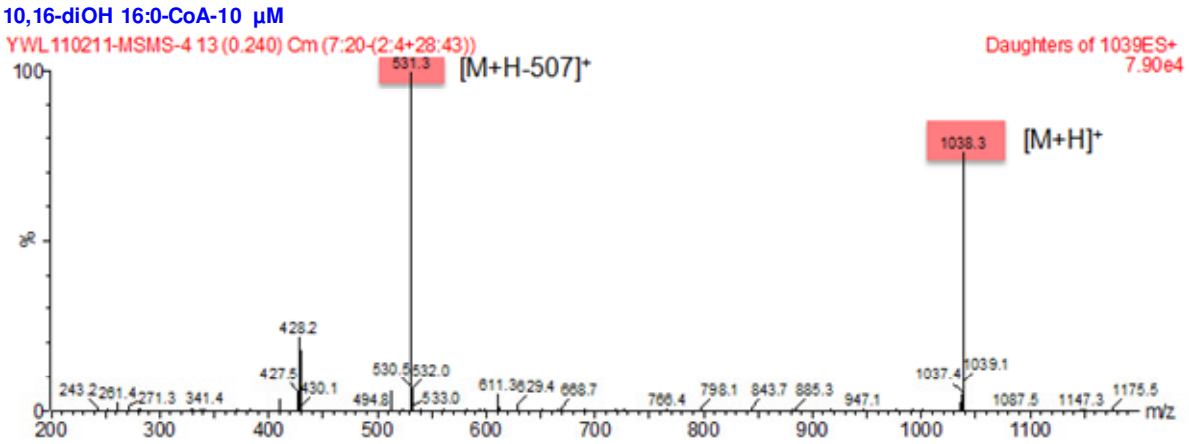

Supplemental Table S1. Identification of ω-OHFA- and DCA-CoAs by ESI-MS/MS. (A) Characteristic fragmentation of protonated acyl-CoA by neutral loss of 507 to give the protonated acyl pantetheine group. Specific *m/z* values observed for $[M+H]^+$ and [acyl pantetheine+H]$^+$ are tabulated. (B) ESI-MS/MS spectrum of 10,16-diOH C16:0-CoA.

Purpose	Primer name	Primer sequence (5′ – 3′)
Yeast expression	GPAT1-cF(pYES2/CT)	CACCAGGATCCATGGTTTTACCAGAGCTTCT
	GPAT1-cR(pYES2/CT)	CACGCAGAATTCTTATCTGACAATGCCTTCATTTCC
Wheat germ expression	GPAT4-cF(pIV1.3WG)	GGAATTCCATATGTCTCCGGCGAAGAAGA (NdeI)
	GPAT4-cR(pIV1.3WG)	TCACCCCGGGTTACTCCATGGACTTGGTCTTATTG (XmaI)
	GPAT8-cF(pIV1.3WG)	CATGCCATGGTTATGTCTCCGGAGAAGAAGAGTCA (NcoI)
	GPAT8-cR(pIV1.3WG)	CCCCCCGGGTCACTTCTTGGTGTTGTTGATAGAC (XmaI)
Screening T-DNA lines	LBa1	TGGTTCACGTAGTGGGCCATCG
	GPAT1-tF	CCGCGGTTACTTACAGCCTA
	GPAT1-tR	TGGACTATACAAATCCAGAAACAA
	GPAT2-tF	CAGAGTCTAGATTCCAGCGACA
	GPAT2-tR	GGGTTTGCCAACTTTTCTTG
	GPAT3-tF	ACGCCACACATTGATCTTCA
	GPAT3-tR	TCGCAATCAAGCAAGTTGTC
	GPAT7-tF	CCTTCGCCTACTTCATGCTC
	GPAT7-tR	TTTTTCATGAACCCGAGACC
Promoter::GUS fusion	pGPAT7-F	CACACAAGCTTCTAAATTATGAAAACATT (EcoRI)
	pGPAT7-R	CACACGGATCCACAACTTAACTTGTTTC (BamHI)
Overexpression	GPAT7-oeF	CACACTCTAGAATGGAGTCATCAACTAC (XbaI)
	GPAT7-oeR	CACACGAGCTCTTAATGCAAAAAAGGTTTG (SacI)

Supplemental Table S2. Primer sequences